Chemoenzymatic synthesis of 2,6-disubstituted tetrahydropyrans with high σ_1 receptor affinity, antitumor and analgesic activity

Nicole Kopp [a], Gianluca Civenni [b], Domenico Marson [c], Erik Laurini [c], Sabrina Pricl [c, d], Carlo V. Catapano [b], Hans-Ulrich Humpf [e], Carmen Almansa [f], Francisco Rafael Nieto [g], Dirk Schepmann [a], Bernhard Wünsch [a, h, *]

[a] *Institut für Pharmazeutische und Medizinische Chemie, Westfälische Wilhelms-Universität Münster, Corrensstraße 48, D-48149, Münster, Germany*
[b] *Institute of Oncology Research, Università della Svizzera Italiana (USI), Via Vincenzo Vela 6, CH-6500, Bellinzona, Switzerland*
[c] *Molecular Biology and Nanotechnology Laboratory (MolBNL@UniTS), DEA, University of Trieste, 34127, Trieste, Italy*
[d] *Department of General Biophysics, Faculty of Biology and Environmental Protection, University of Lodz, Lodz, Poland*
[e] *Institut für Lebensmittelchemie, Westfälische Wilhelms-Universität Münster, Corrensstraße 45, D-48149, Münster, Germany*
[f] *Esteve Pharmaceuticals S.A., Baldiri Reixach 4-8, 08028, Barcelona, Spain*
[g] *Department of Pharmacology and Neurosciences Institute (Biomedical Research Center), University of Granada and Biosanitary Research Institute, 18010, Granada, Spain*
[h] *GRK 2515, Chemical Biology of Ion Channels (Chembion), Westfälische Wilhelms-Universität Münster, Germany*

ARTICLE INFO

Keywords:
σ_1 receptor
2,6-Disubstituted tetrahydropyrans
Chemoenzymatic synthesis
Stereochemistry
Kinetic resolution
Chiral HPLC
CD spectroscopy
σ_1 receptor affinity
Selectivity
Structure affinity relationships
Docking studies
Molecular dynamics
Steered molecular dynamics
Antitumor activity
Androgen negative human prostate cancer cell line DU145
Neuropathic pain
Analgesic activity
Antiallodynic activity

ABSTRACT

1,3-Dioxanes **1** and cyclohexanes **2** bearing a phenyl ring and an aminoethyl moiety in 1,3-relationship to each other represent highly potent σ_1 receptor antagonists. In order to increase the chemical stability of the acetalic 1,3-dioxanes **1** and the polarity of the cyclohexanes **2**, tetrahydropyran derivatives **3** equipped with the same substituents were designed, synthesized and pharmacologically evaluated. The key step of the synthesis was a lipase-catalyzed enantioselective acetylation of the alcohol (*R*)-**5** leading finally to enantiomerically pure test compounds **3a**-**g**. With respect to σ_1 receptor affinity and selectivity over a broad range of related (σ_2, PCP binding site) and further targets, the enantiomeric benzylamines **3a** and cyclohexylmethylamines **3b** represent the most promising drug candidates of this series. However, the eudismic ratio for σ_1 binding is only in the range of 2.5−3.3. Classical molecular dynamics (MD) simulations confirmed the same binding pose for both the tetrahydropyran **3** and cyclohexane derivatives **2** at the σ_1 receptor, according to which: i) the protonated amino moiety of (2*S*,6*R*)-**3a** engages the same key polar interactions with Glu172 (ionic) and Phe107 (π-cation), ii) the lipophilic parts of (2*S*,6*R*)-**3a** are hosted in three hydrophobic regions of the σ_1 receptor, and iii) the O-atom of the tetrahydropyran derivatives **3** does not show a relevant interaction with the σ_1 receptor. Further *in silico* evidences obtained by the application of free energy perturbation and steered MD techniques fully supported the experimentally observed difference in receptor/ligand affinities. Tetrahydropyrans **3** require a lower dissociative force peak than cyclohexane analogs **2**. Enantiomeric benzylamines **3a** and cyclohexylmethylamines **3b** were able to inhibit the growth of the androgen negative human prostate cancer cell line DU145. The cyclohexylmethylamine (2*S*,6*R*)-**3b** showed the highest σ_1 affinity ($K_i(\sigma_1) = 0.95$ nM) and the highest analgesic activity *in vivo* (67%).

1. Introduction

The unique class of σ receptors, which was originally regarded as subtype of the opioid receptor class, contains σ_1 and σ_2 receptor subtypes[1–4]. In addition to its expression in the central nervous

* Corresponding author. Institut für Pharmazeutische und Medizinische Chemie, Westfälische Wilhelms-Universität Münster, Corrensstraße 48, D-48149, Münster, Germany.
E-mail address: wuensch@uni-muenster.de (B. Wünsch).

system (CNS), σ_1 receptors are also found in various peripheral organs such as liver, heart, kidney, and lung[4–8].

Due to their localization in the CNS, σ_1 receptors play a key role in various neuropsychiatric disorders including depression, schizophrenia and drug/alcohol dependence[9–14]. Although the phenotype of σ_1 receptor knock-out mice is rather normal, they show depression-like behavior[15,16]. Moreover, several antidepressants in clinical use interact with medium to high affinity with σ_1 receptors [14,17,18]. In addition, σ_1 receptors are involved in neurodegenerative disorders, like Alzheimer's disease. σ_1 agonistic activity contributes considerably to the neuroprotective effects of the anti-Alzheimer drug donepezil inhibiting the acetylcholine esterase[19,20]. It has been shown that σ_1 receptors can be used for the treatment of neuropathic pain. Thus, the pyrazole derivative S1RA developed by Esteve has been studied in phase II of clinical trials for the treatment of neuropathic pain[21,22]. With respect to analgesic activity in neuropathic pain mouse models, pain-like behaviors, such as allodynia, are attenuated in σ_1 knockout mice and in wild-type animals treated with σ_1 receptor antagonists[21–23]. Capsaicin-induced mechanical allodynia is considered a surrogate model of neuropathic pain [24,25] allowing the differentiation of σ_1 ligands into agonists [26] and antagonists[24]. σ_1 Receptor ligands displaying analgesic activity in the capsaicin assay are regarded as σ_1 receptor antagonists[21,24].

In addition to the localization of σ_1 receptors in the CNS, high expression levels of σ_1 receptors were detected across several human tumor types, *e.g.* prostate, lung, bladder, and breast tumors. Treatment of these tumor cells with σ_1 receptor antagonists resulted in reduced tumor cell proliferation and survival. The high expression level of σ_1 receptors in tumors can be associated with strong metastasis and a poor prognosis for the patients[27,28].

Although the σ_1 receptor gene was already cloned approx. 25 years ago[29–33], the 3D structure of this unique receptor could not be identified until 2016, when A. Kruse and coworkers reported for the first time the X-ray crystal structure of the σ_1 receptor in complex with two structurally divergent ligands (PD144418 and 4-IBP)[34]. Two years later, the structures of the σ_1 receptor in complex with the prototypical σ_1 receptor antagonists haloperidol and NE-100 and with the prototypical agonist (+)-pentazocine were published[35]. This effort revealed that an ionic interaction between the receptor residue Glu172 and the protonated cationic amino moiety of the ligands represents a key interaction in both structure types. In 2017, the σ_2 receptor was isolated from calf liver tissue and identified as the endoplasmic reticulum (ER)-resident transmembrane protein 97 (TMEM97)[36]. In contrast to the σ_1 receptor, the human σ_2 receptor was not crystallized so far.

Herein, we report on the design, synthesis and pharmacological evaluation of novel σ_1 receptor ligands, which should target single tumor cells, bulk tumors and, furthermore, tumor stem cells. Ligands interacting with σ_1 receptors exhibit a large structural diversity[13,37,38]. Recently, we have shown that racemic 1,3-dioxane **1** with a benzylaminoethyl moiety in 4-position displays high σ_1 receptor affinity ($K_i(\sigma_1) = 19$ nM [39] and high antiallodynic activity *in vivo* in the mouse capsaicin assay confirming σ_1 antagonistic activity of **1**[40]. For the pure enantiomer (2*S*,4*R*)-**1**, an even higher σ_1 receptor affinity ($K_i = 6.0$ nM) was found[41]. (Fig. 1).

The high σ_1 receptor affinity and antiallodynic activity of 1,3-dioxane **1** prompted us to further investigating this compound class. In particular, the acetalic substructure of **1** can be hydrolyzed rapidly under acidic conditions (*e.g.* stomach). Therefore, the 1,3-dioxane ring of **1** was replaced by a cyclohexane ring (**2**). The (1*R*,3*S*)-configured cyclohexane (1*R*,3*S*)-**2a** (NR_2 = NHBn), whose structure corresponds to the structure of 1,3-dioxane (2*S*,4*R*)-**1**, exhibited very high σ_1 receptor affinity ($K_i(\sigma_1) = 0.6$ nM). The enantiomer (1*S*,3*R*)-**2a** showed comparably high σ_1 receptor affinity ($K_i(\sigma_1) = 1.3$ nM)[42]. (Fig. 1).

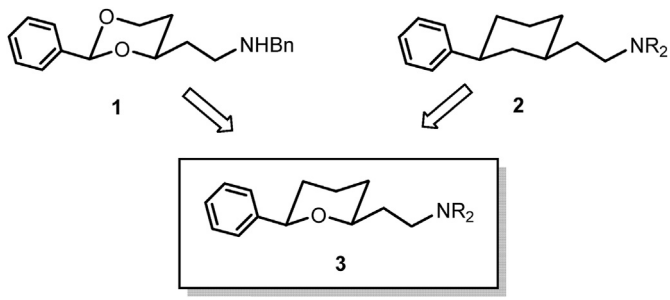

Fig. 1. Design of (tetrahydropyranyl)ethanamines **3** as compromise between 1,3-dioxanes **1** (acid lability) and cyclohexanes **2** (high lipophilicity).

Table 1
Calculated $clogD_{7.4}$ values of **1**, **2a** (NR_2 = NHBn), and **3a** (NR_2 = NHBn).

compd.	$clogD_{7.4}$[a)] calcd. with ChemAxon
1	1.30
2a (NR_2 = NHBn)	3.10
3a (NR_2 = NHBn)	2.05

However, replacement of the 1,3-dioxane ring of **1** by the cyclohexane ring in **2** raised the lipophilicity remarkably. The calculated (ChemAxon) $clogD_{7.4}$ value of **2a** (NR_2 = NHBn) is 3.10, which is considerably higher than the $clogD_{7.4}$ value of the 1,3-dioxane **1** ($clogD_{7.4}$ = 1.30). The $clogD_{7.4}$ value of **2a** (NR_2 = NHBn, $clogD_{7.4}$ = 3.10) correlates nicely with the $logD_{7.4}$ value of 3.13 experimentally determined by the micro-shake-flask method[42–44]. (Table 1).

In order to conserve the high σ_1 receptor affinity of the 1,3-dioxane **1** and cyclohexanes **2** the six-membered core system should be maintained. To reduce the hydrolytic lability of acetal **1** and the high lipophilicity of cyclohexane **2**, the tetrahydropyran derivatives of type **3** with only one O-atom within the six-membered ring were envisaged. Due to removal of one CH_2-moiety of **2a** by one O-atom in **3a** (NR_2 = NHBn) the calculated $clogD_{7.4}$ value was reduced to 2.05 indicating higher polarity of tetrahydropyrans **3**. In contrast to the 1,3-dioxane **1**, tetrahydropyran derivatives **3** cannot be hydrolyzed any more by acids.

2. Results and discussion

2.1. Synthesis

At first, a synthesis providing racemic pyranylethanamines of type **3** was established (Scheme 1). δ-Oxoester **4** was reduced with $NaBH_4$ to yield the δ-hydroxyester **5**, which was cyclized with trifluoroacetic acid to give the δ-lactone **7**. In order to get a reference compound for the planned kinetic resolution by enantioselective acetylation using lipases as catalysts, the acetate **6** was prepared by acetylation of the alcohol **5** with acetic anhydride.

Reduction of δ-lactone **7** with diisobutylaluminum hydride (DIBAL) led to the hemiacetal **8** as mixture of two diastereomers. In the next reaction step, the lactol (hemiacetal) **8** underwent a Domino reaction with the stabilized P-Ylid $Ph_3P{=}CHCO_2CH_3$. After opening of the lactol **8** to give a δ-hydroxyaldehyde, a Wittig reaction occurred with the aldehyde affording the α,β-unsaturated ester **9**, which was cyclized with KO^{t}Bu *via* an intramolecular conjugate addition. The cyclization of the α,β-unsaturated ester **9** occurred under thermodynamically controlled reaction conditions leading exclusively to the thermodynamically favored *cis*-configured diastereomer **10** (Scheme 1).

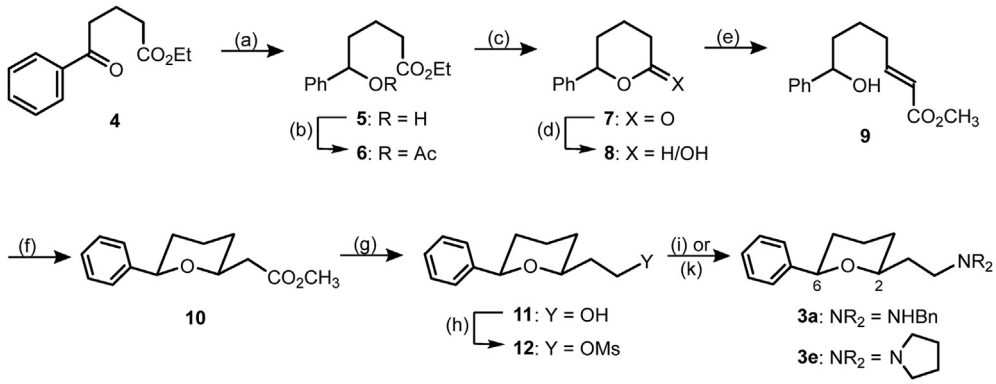

Scheme 1. Synthesis of racemic amines **3a** and **3e**. Reagents and reaction conditions: (a) $NaBH_4$, EtOH, rt, 6 h, 67%. (b) Ac_2O, NEt_3, THF, 66 °C, 29 h, 40%. (c) **5**: F_3CCO_2H, CH_2Cl_2, rt, 24 h, 72%. (d) DIBAL, CH_2Cl_2, toluene, −78 °C, 1 h, 86%. (e) $Ph_3P{=}CHCO_2CH_3$, THF, 66 °C, 5.5 h, 27%. (f) KO^tBu, THF, rt, 23 h, 44%. (g) $LiAlH_4$, THF, rt, 2 h, 91%. (h) CH_3SO_2Cl, CH_2Cl_2, NEt_3, rt, 16 h, 90%. (i) $BnNH_2$, CH_3CN, 82 °C, 19 h, 75% (**3a**). (k) Pyrrolidine, CH_3CN, 82 °C, 19 h, 90% (**3e**). All compounds in Scheme 1 represent racemic mixtures.

The relative *cis*-configuration of the ester **10** was confirmed by a nuclear Overhauser effect (NOE) experiment. Irradiation with the resonance frequency of 2-H_{ax} at 3.98 ppm resulted in an increased signal at 4.41 ppm (6-H_{ax}). Vice versa, irradiation at 4.41 ppm (6-H_{ax}) led to an increased signal at 3.98 ppm (2-H_{ax}). (NOE spectra of **10** in Supporting Information) The influence of these signals on each other indicates a close proximity of the corresponding protons, i.e. *cis*-orientation at the cyclohexane ring.

$LiAlH_4$ reduction of the ester **10** led to the primary alcohol **11** in 91% yield. Activation of the alcohol **11** with methanesulfonyl chloride yielded the mesylate **12**, which was substituted by primary and secondary amines, such as benzylamine and pyrrolidine, giving the amines **3a** and **3e**, respectively.

2.2. Stereochemistry

Since the racemic amines (±)-**3a** and (±)-**3e** showed promising σ_1 receptor affinity, the synthesis of enantiomerically pure amines of type **3** was planned. To this purpose, a kinetic resolution of the racemic alcohol (±)-**5** using lipases as chiral catalysts was envisaged. In order to evaluate the quality of the lipase-catalyzed transformation chiral HPLC methods were established to separate the enantiomers of the alcohol (±)-**5** and the acetate (±)-**6**. With the chiral stationary phase Chiralcel OD-H the enantiomers of both the alcohol (±)-**5** and the acetate (±)-**6** could be separated (Figures S1 and S2 in Supporting Information).

Standard reaction conditions for the first screening: room temperature, 200 mg of racemic alcohol (±)-**5**, 20 mL of *tert*-butyl methyl ether, 300 mg of lipase or 200 mg of immobilized lipase, 5 equivalents of isopropenyl acetate.

After establishment of the required HPLC methods, the performance of eight lipases was screened under standard conditions. The name of the used lipase, the organism producing this lipase and the type of preparation are summarized in Table S2 in Supporting Information. The alcohol (±)-**5** was reacted with isopropenyl acetate in *tert*-butyl methyl ether (TBME) at room temperature using one of the listed lipases as catalyst. The results are summarized in Table 2.

The best results were obtained using *Burkholderia cepacia* lipase as powder (experiment **F**), immobilized on ceramic particles (experiment **G**) or immobilized on diatomaceous earth (experiment **H**) leading to (*R*)-configured acetate (*R*)-**6** in high yields. In order to find the optimal time point to stop the reaction catalyzed by Amano Lipase PS-CII, the development of the transformation and the ee-value for (*S*)-configured alcohol (*S*)-**5** were recorded by HPLC analysis of samples taken at different time points. After 76 h, alcohol (*S*)-**5** was obtained with 98.4% ee and 48% yield. A longer reaction time led to further increase of the ee-value of (*S*)-**5**, but also to reduced amounts of the alcohol (*S*)-**5** (Figure S3 in Supporting Information). Simulation of this transformation [45] led to an enantioselectivity of 50 : 1, i.e. (*R*)-configured alcohol (*R*)-**5** was acetylated 50-fold faster than (*S*)-configured alcohol (*S*)-**5** (Figure S4 in Supporting Information).

Table 2
Results obtained in the screening of various lipases to achieve a kinetic resolution of racemic alcohol (±)-**5**.

lipase[a)]	time [h]	yield 5 mg/%	ratio (*S*)-5: (*R*)-5	yield 6 mg/%	ratio (*R*)-6: (*S*)-6
A	170	179/90	51.9 : 48.1	4/2	94.9 : 5.1
B	213	164/82	53.3 : 46.7	16/7	93.4 : 6.6
C	145	126/63	41.1 : 58.9	33[a)]/21	13.1[b)]: 86.9[b)]
D	90	115/57	44.9 : 55.1	42[a)]/26	20.8[b)]: 79.2[b)]
E	141	149/74	56.5 : 43.5	26/11	96.1 : 3.9
F	165	161/80	57.6 : 42.4	29/12	97.8 : 2.2
G	20	114/57	78.7 : 21.3	82/34	97.2 : 2.8
H	20	129/64	67.8 : 32.2	57/24	97.9 : 2.1

[a)] **A**: lipase from *Candida rugosa*; **B**: Chirazyme L-3; **C**: Lipozyme; **D**: Chirazyme L-7; **E**: Amano lipase AK; **F**: Amano Lipase PS; **G**: Amano Lipase PS—CII; **H**: Amano Lipase PS-IM.
[b)] The enantioselectivity was turned around, i.e. (*S*)-**5**-was acetylated preferably.

In order to obtain a large amount of enantiomerically pure alcohol (*S*)-**5**, a large amount of racemic alcohol (±)-**5** (7.59 g) was reacted with isopropenyl acetate in the presence of the immobilized Amano Lipase PS-IM. Due to the high quantity of substrate and reagents, the endpoint of the reaction was determined experimentally. After 144 h, the alcohol (*S*)-**5** was obtained with 99.4% ee and 41% yield, whereas the acetate (*R*)-**6** was isolated in 49% yield with an enantiomeric excess of 78.1% ee (Scheme 2).

The enantiomeric alcohol (*R*)-**5** was prepared starting from the enantiomerically enriched acetate (*R*)-**6** (78.1% ee) (Scheme 3). Ethanolysis of the acetate (*R*)-**6** led to the (*R*)-configured alcohol (*R*)-**5** (78.1% ee), which was again acetylated with isopropenyl acetate in the presence of Amano lipase PS-IM. However, this time, the transformation was stopped already after 84 h resulting in the acetate (*R*)-**6** in 98.8% ee and 82% yield. As a side product (*S*)-**5** was obtained with a low ee value. A second ethanolysis of (*R*)-**6** afforded enantiomerically pure alcohol (*R*)-**5** (98.8% ee, 88% yield). Although the synthesis of enantiomeric alcohols (*R*)-**5** (methyl ester, 83% ee) and (*S*)-**5** (90% ee) has already been described in literature by enantioselective CBS reduction and DIP-Cl reduction of δ-oxoester **4** [46,47], respectively, the enantiomeric excess obtained herein by lipase catalyzed kinetic resolution is considerably higher than the reported ee values.

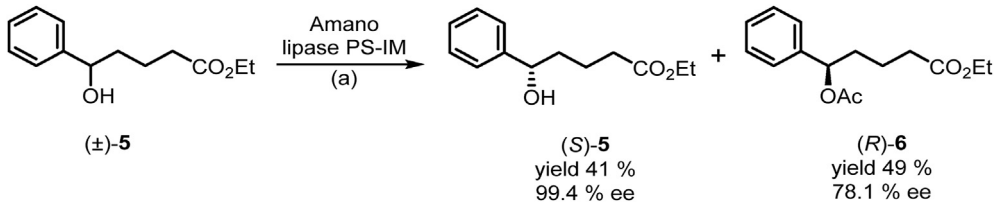

Scheme 2. Kinetic resolution of racemic alcohol (±)-**5**. Reagents and reaction conditions: (a) Isopropenyl acetate, Amano lipase PS-IM, TBME, rt, 144 h.

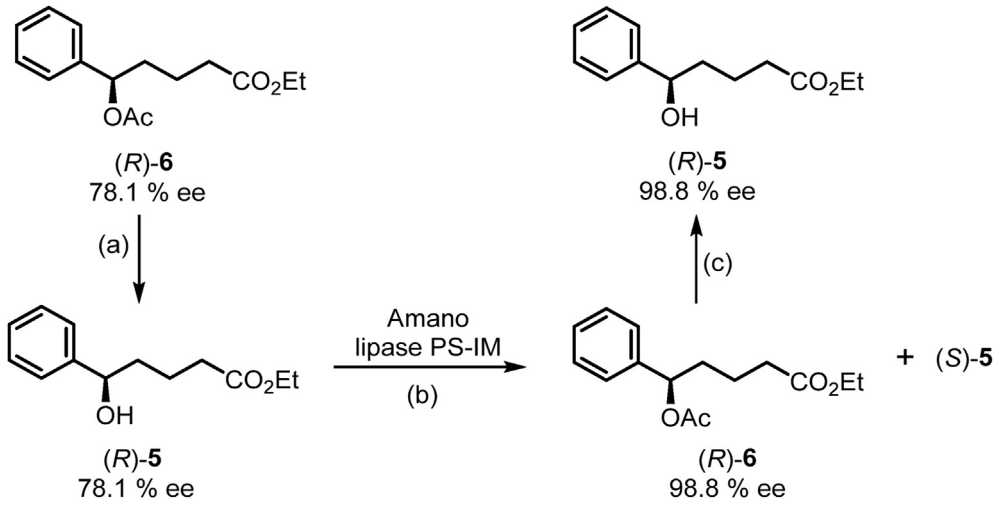

Scheme 3. Synthesis of enantiomerically pure alcohol (R)-**5**. Reagents and reaction conditions: (a) EtOH, K_2CO_3, rt, 15.5 h, 82%. (b) Isopropenyl acetate, Amano lipase PS-IM, TBME, rt, 84 h, 82%. (c) EtOH, K_2CO_3, rt, 22 h, 88%.

The enantiomeric amines (2S,6R)-**3a**-**f** and (2R,6S)-**3a**-**f** were prepared in the same manner as the racemic benzylamine (±)-**3a** and pyrrolidine (±)-**3e** (Scheme 4). Key intermediates of this synthesis are the enantiomerically pure mesylates (2S,6R)-**12** and (2R,6S)-**12** allowing the introduction of diverse amino moieties at the very end of the synthesis (late stage diversification). Nucleophilic substitution with primary and secondary amines yielded various secondary **3a**-**c** and tertiary amines **3d**-**f**. The primary amines **3g** were obtained by hydrogenolytic cleavage of the benzylamines **3a**.

The lactones (*R*)-**7** and (*S*)-**7** represent the first products formed by intramolecular transesterification of the δ-hydroxyesters (*R*)-**5** and (*S*)-**5**. There are already some reports on the preparation of the lactones (*R*)-**7** and (*S*)-**7**. For example, chromatographic separation of racemic lactone (±)-**7** led to the pure enantiomers[48]. According to a second method, the alcohol (*S*)-**5** was prepared by DIP-Cl reduction of ketone **4** and was subsequently cyclized to give the lactone (*S*)-**7**[47,49]. In some reports only 50% ee was reported [50,51]. Additionally, two kinetic resolutions of racemic mixtures using enzymes have been reported. In the first report, racemic 1-phenylpentane-1,5-diol was acetylated with isopropenyl acetate in the presence of Amano Lipase PS-CII leading to enantiomeric 5-monoacetate and 1,5-diacetate, which were further proceeded[52]. In the second approach, racemic lactone (±)-**7** was hydrolyzed

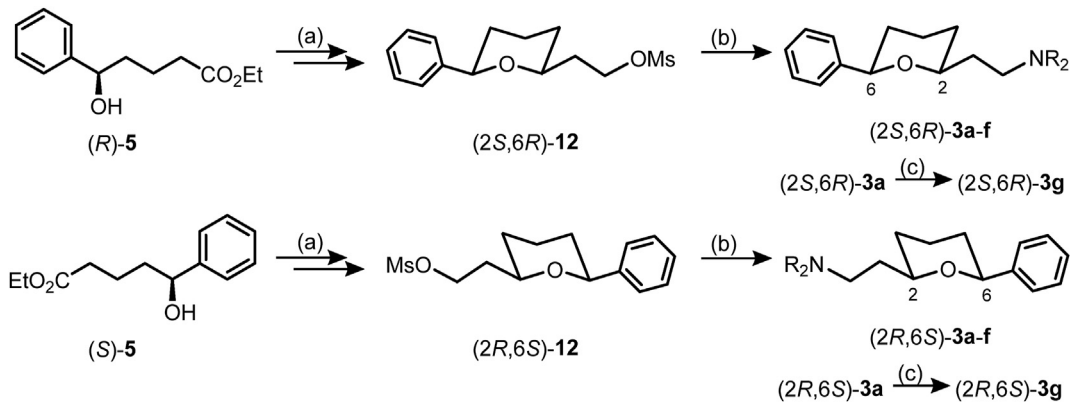

Scheme 4. Synthesis of enantiomerically pure amines (2S,6R)- **3a**-**f** and (2R,6S)-**3a**-**f**. Reagents and reaction conditions: (a) six reaction steps, see Scheme 1. (b) R_2NH, CH_3CN, 82 °C, 13–21 h, 50–93%, **3a**: NR_2 = NHBn; **3b**: NR_2 = $NHCH_2C_6H_{11}$; **3c**: NR_2 = $NH(CH_2)_4Ph$; **3d**: NR_2 = $N(CH_3)_2$; **3e**: NR_2 = pyrrolidino; **3f**: NR_2 = 4-phenylpiperazin-1-yl. (c) H_2 (5 bar), Pd/C, THF, 2 × 20 h, rt, 42–61%, **3g**: NR_2 = NH_2.

enantioselectively with horse liver esterase in a buffer system resulting in lactone (*S*)-**7** and (*R*)-configured hydroxy acid in 50% ee, respectively[53].

After establishment of the second center of chirality in 2-position, the enantiomeric purity of the 2,6-disubstituted tetrahydropyrans was verified. For this purpose, a chiral HPLC method for the separation of the enantiomers of primary alcohol **11** was developed. Using an OH−H chiral stationary phase led to base-line separation of alcohols (2*S*,6*R*)-**11** and (2*R*,6*S*)-**11**/see Figure S5 in Supporting Information). This method led to ee values of 98.0% ee and 98.3% ee for the enantiomeric alcohols (2*S*,6*R*)-**11** and (2*R*,6*S*)-**1**, respectively. Thus, racemization during the synthesis of primary alcohols (2*S*,6*R*)-**11** and (2*R*,6*S*)-**11** can be excluded.

CD spectra of the enantiomeric benzylamines (2*S*,6*R*)-**3a** and (2*R*,6*S*)-**3a** were recorded to analyze the absolute configuration of the final ethanamines **3** and their synthetic intermediates (Fig. 2). The recorded CD spectra of the enantiomers (2*S*,6*R*)-**3a** and (2*R*,6*S*)-**3a** are mirror images to each other showing a positive and a negative Cotton effect at approx. 215 nm, respectively. A positive Cotton effect at 215 nm was also found by calculating the CD spectrum of the model compound (2*R*,6*R*)-2-methyl-6-phenyltetrahydropyran (see Figure S6 in Supporting Information). Replacing the conformationally flexible benzylaminoethyl side chain by the small methyl moiety was necessary to reduce the number of possible conformations to be considered during the calculation. However, introduction of the methyl moiety led to a change of the stereodescriptor in 2-position. The calculated CD spectrum of the model compound nicely confirms the (2*S*,6*R*)-configuration of enantiomer (2*S*,6*R*)-**3a**. Moreover, the recorded CD spectra nicely correlate with the CD-spectra recorded for the analogous cyclohexane derivatives (1*R*,3*S*)-**2a** and (1*S*,3*R*)-**2a** (NR_2 = NHBn) [42].

The same assignment of the absolute configuration was obtained applying the rule of Kaslauskas [54]. According to this rule a lipase preferably transforms the (*R*)-enantiomer of a secondary alcohol provided that the larger substituent has the higher priority according to the CIP rules. In case of the secondary alcohol **5**, the phenyl moiety is larger than the alkyl chain and has the higher priority according to the CIP rules. Therefore, the Amano Lipase PS-IM acetylated selectively the (*R*)-configured enantiomer leaving the (*S*)-enantiomer unchanged. Correlation of the specific optical rotation of the synthesized compounds (*R*)-**5**, (*S*)-**5**, (*R*)-**7**, and (*S*)-**7** with those of the compounds already reported in literature resulted in the same assignment of the absolute configuration. This assignment was additionally supported by comparison of the specific optical rotation of the enantiomerically pure lead compounds **1** and **2a** with those of the newly synthesized tetrahydropyrans **3a**.

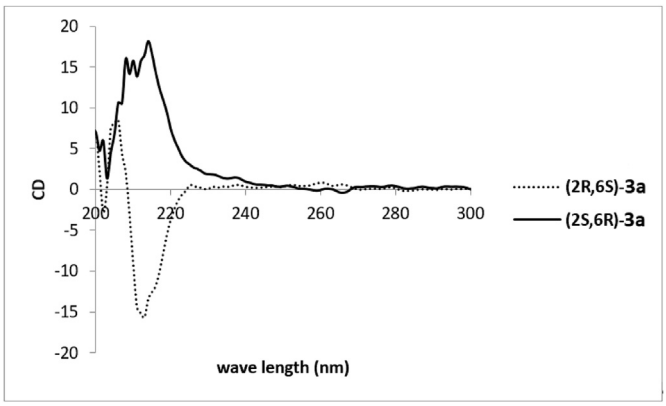

Fig. 2. CD spectra (CH_3CN) of enantiomeric benzylamines (2R,6S)-**3a** and (2S,6R)-**3a**.

2.3. Receptor affinity

Competitive radioligand receptor binding studies were performed to determine the σ_1 and σ_2 receptor affinity of the tetrahydropyran derivatives **3**. In the σ_1 assay, tritium labeled [^{3}H](+)-pentazocine and guinea pig brain membrane preparations were used, whereas rat liver membrane preparations and the radioligand [^{3}H]di-*o*-tolylguanidine were employed in the σ_2 assay [55−57]. In Table 3, σ_1 and σ_2 receptor affinities of (tetrahydropyranyl)ethanamines **3** are summarized and compared with the affinities of some reference compounds.

Compared with the analogous cyclohexane derivatives **2** [42], substituents at the amino moiety of the tetrahydropyran derivatives **3** have a stronger impact on the σ_1 affinity. The highest σ_1 affinity was detected for the benzylamines **3a** and cyclohexylmethylamines **3b**, with (2*S*,6*R*)-configured cyclohexylmethylamine (2*S*,6*R*)-**3b** possessing the highest K_i value (K_i = 0.95 nM) in this series of compounds. Extension of the side chain from one CH_2 moiety (**3a**) to four CH_2 moieties (**3c**) resulted in 5- to 10-fold decreased σ_1 affinity. A further reduction of σ_1 affinity was observed for the tertiary amines bearing a pyrrolidino (**3e**) and phenylpiperazino moiety (**3f**). The dimethylamine **3d** with two small methyl moieties attached at the amino group showed low σ_1 affinity in the high nanomolar range, whereas the primary amine **3g** was even less potent.

The absolute configuration had only a low influence on the σ_1 affinity. Generally, the eudismic ratio is in the range of 2.0−3.3 with (2*S*,6*R*)-configured enantiomers being the eutomers. The dimethylamines **3d** and pyrrolidines **3e** were recognized as the only exceptions of this rule, as (2*R*,6*S*)-**3d** and (2*R*,6*S*)-**3e** represent the eutomers with eudismic ratios of 2.1 and 1.9, respectively.

Except for the cyclohexylmethylamines **3b**, the σ_2 affinity of the amines **3** is rather low (K_i > 100 nM). Thus in particular the benzylamine (2*S*,6*R*)-**3a** ($K_i(\sigma_1)$ = 1.6 nM) exhibits an excellent 236-fold selectivity for σ_1 receptors over σ_2 receptors. Although the cyclohexylmethylamine (2*S*,6*R*)-**3b** shows an even higher σ_1 affinity ($K_i(\sigma_1)$ = 0.95 nM), its σ_1/σ_2 selectivity is reduced to 60-fold due to increased σ_2 affinity. The eudismic ratio concerning the σ_2 affinity is also very low (1.1−1.6) indicating low influence of the absolute configuration on the σ_2 affinity.

As 1,3-dioxane derivatives of type **1** with a primary amino moiety display high affinity towards the phencyclidine (PC) binding site within the NMDA receptor associated ion channel [41], the affinity of the tetrahydropyran derivatives **3** towards the PCP binding site was also recorded in receptor binding studies. However, even at the very high test compound concentration of 1 μM, the amines **3** could not compete with the radioligand [^{3}H](+)MK-801 for the PCP binding site. According to this result, the investigated amines display high selectivity for σ_1 receptors over the PCP binding site at the NMDA receptor.

In a small screening, the benzylamines (2*R*,6*S*)-**3a** and (2*S*,6*R*)-**3a** as well as the cyclohexylmethylamines (2*R*,6*S*)-**3b** and (2*S*,6*R*)-**3b** did not interact with human serotoninergic 5-HT_{1A}, 5-HT_{2B}, adrenergic α_{1A}, α_{2A}, and opioid receptors MOR, DOR, KOR. Moreover, inhibition of noradrenalin, serotonin and dopamine transporters was not observed. At a concentration of 1 μM, the CYP enzymes CYP1A2, CYP2C9, CYP2C19, and CYP3A4 were not inhibited.

2.4. Computational studies on σ_1 receptor binding

The pose of the amines **3** in the binding site of the σ_1 receptor was analyzed starting with the structure of the σ_1 receptor reported in the RCSB Protein Data Bank (PDB ID 5HK1) [34]. Inspection of the binding mode of the newly synthesized tetrahydropyran

Table 3
Affinities of prepared (tetrahydropyranyl)ethanamines **3** towards σ_1 and σ_2 receptors as well as towards the PCP binding site of the NMDA receptor.

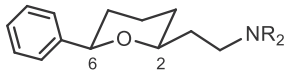

compd.	-NR_2	K_i ± SEM [nM] (n = 3)				
		σ_1	eudismic ratio	σ_2	eudismic ratio	PCP
(2*R*,6*S*)-**3a**	NHBn	5.4 ± 0.87	3.3	426[b)]	1.1	
(2*S*,6*R*)-**3a**		1.6 ± 0.17		378[b)]		
(2*R*,6*S*)-**3b**	$NHCH_2C_6H_{11}$	2.4 ± 1.2	2.5	36 ± 11	1.6[c)]	7%
(2*S*,6*R*)-**3b**		0.95 ± 0.60		57 ± 23		33%
(2*R*,6*S*)-**3c**	$NH(CH_2)_4Ph$	29 ± 7.6	2.0	377[b)]	1.6	42%
(2*S*,6*R*)-**3c**		15 ± 5.0		234 ± 35		43%
(2*R*,6*S*)-**3d**	$N(CH_3)_2$	217 ± 6.0	2.1[c]	4000 ± 600	1.7	31%
(2*S*,6*R*)-**3d**		465 ± 15		2300 ± 300		37%
(2*R*,6*S*)-**3e**		31 ± 9.1	1.9[c)]	170[b)]	1.5	
(2*S*,6*R*)-**3e**		60 ± 9		115[b)]		
(2*R*,6*S*)-**3f**		57 ± 16	2.7	161 ± 59	1.2	
(2*S*,6*R*)-**3f**		21 ± 5.7		131 ± 44		7%
(2*R*,6*S*)-**3g**	NH_2	4 %[a)]	–	10 %[a)]	–	43%
([a]2*S*,6*R*)-**3g**		9 %[a)]		5 %[a)]		14 %
(+)-pentazocine		5.7 ± 2.2		–		
Haloperidol		6.3 ± 1.6		78 ± 2.3		
di-*o*-tolylguanidine		89 ± 29		58 ± 18		

The given K_i values represent means of three independent experiments (n = 3).
[a] Values in % represent the inhibition of the radioligand binding at a test compound concentration of 1 μM.
[b] Values without SEM represent the mean of two experiments.
[c] In contrast to all other pairs of enantiomers, the dimethylamine (2*R*,6*S*)-**3d** and pyrrolidine (2*R*,6*S*)-**3e** represent the eutomer, i.e. the eudismic ratios of 2.1 and 1.9 for σ_1 affinity refers to (2*R*,6*S*)-configured enantiomers as eutomers.

derivatives **3** in the σ_1 receptor cavity *via* our consolidated Molecular Dynamics (MD) simulation protocol clearly revealed that these tetrahydropyran derivatives **3** share highly similar binding poses and interaction patterns as the corresponding cyclohexane derivatives **2** [42]. Taking compound (2*S*,6*R*)-**3a** as a proof-of-principle, the equilibrated MD snapshot shown in Fig. 3A confirms that the 7 performed by the protonated nitrogen atom of (2*S*,6*R*)-**3a** are required to foster the peculiar binding specific polar interaction with E172 and the π-cation interaction with the side chain of F107 of these derivatives. Furthermore, the present simulations also confirm the stabilizing effect of the hydrogen bond between E172 and Y103. Interestingly, as in the case of the other two molecules synthesized previously, the prevalently lipophilic scaffold of (2*S*,6*R*)-**3a** can be suitably hosted in three σ_1 receptor hydrophobic regions. Specifically, the N-benzyl ring is engaged in favorable van der Waals interactions with the hydrocarbon side chain of I124 while the other aromatic ring and the tetrahydropyranyl moiety are nested in a receptor cavity formed by residues L105, T181, and A185 and the other hydrophobic cleft lined by the side chains of L182, L186, T202, and Y206.

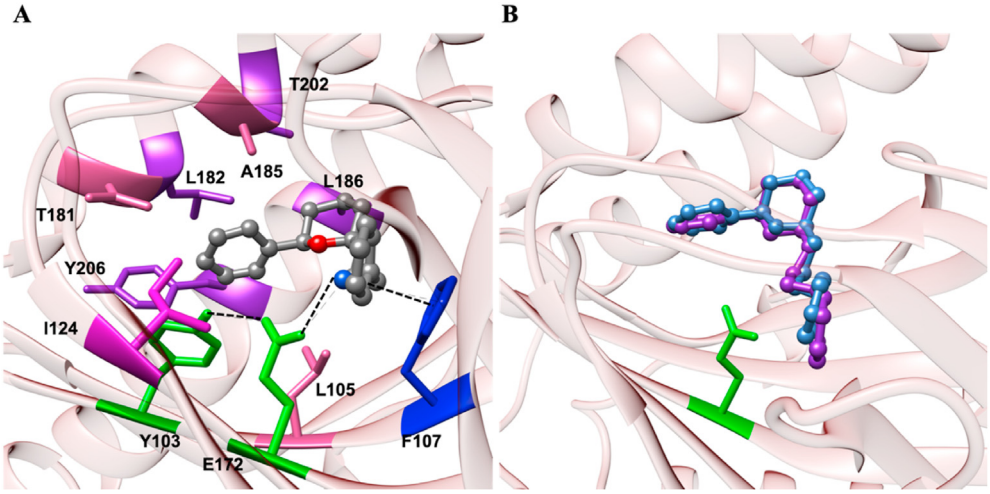

Fig. 3. (A) Details of compound (2*S*,6*R*)-**3a** in the binding pocket of the σ_1 receptor. The ligand is shown as atom-colored sticks-and-balls (C, grey, N, blue, O, red) while the side chains of the mainly interacting residues are represented as colored sticks and labeled. Hydrogen atoms, water molecules, ions, and counterions are omitted for clarity. (B) Overlay of σ_1 binding modes of compound (2*S*,6*R*)-**3a** (cornflower blue) and its cyclohexyl derivative (1*R*,3*S*)-**2a** (NR_2 = NHBn, purple).

It is worth to mention here that the O-atom in the tetrahydropyran ring seems to be dispensable for σ_1 receptor binding. Indeed, according to the relevant MD simulations this atom does not appear to be involved in any particular interaction with σ_1 residues while, at the same time, it does not interfere with the binding pose, as demonstrated by the perfect superimposition between (2*S*,6*R*)-**3a** and its corresponding cyclohexane analog (1*R*,3*S*)-**2a** (NR_2 = NHBn) shown in Fig. 3B.

Based on these MD-based docking results, the slightly higher σ_1 receptor affinity of the cyclohexane derivatives **2** compared with the new tetrahydropyran-based compounds could be hardly explained. Accordingly, in trying to support the experimentally observed decrease of affinity for the tetrahydropyran derivatives with *in silico* techniques we resorted to free energy perturbation (FEP) calculations implemented in AMBER19 software [58]. Accordingly, we carried out FEP simulations of the σ_1 receptor in complex with the *(2S,6R)*-configured enantiomers of **3a** and **3c-g**. Contextually, the same computational protocol was applied to the cyclohexane derivatives **2** bearing the same $-NR_2$ substituent for comparison. All FEP data - expressed as binding free energy difference $\Delta\Delta G_{FEP} = \Delta G_{FEP}$(**2**-derivative) $- \Delta G_{FEP}$(**3**-derivative) - consistently yielded negative, *i.e.*, unfavorable $\Delta\Delta G_{FEP}$ values for the newly synthetized compounds (Fig. 4A). Notably, the calculated relative binding free energies are in very good agreement with the relevant experimental $\Delta\Delta G_{exp}$ as calculated from the corresponding K_i values, as also shown in Fig. 4A and B.

To further investigate the different behavior of the two series of compounds **2** and **3**, we derived the force profile for the unbinding event of each ligand from the σ_1 receptor *via* steered molecular dynamics (SMD) simulations. Interestingly, the SMD results nicely correlate with the σ_1 affinity values experimentally determined for both series of compounds (K_i-values in Table 3), *i.e.*, the lower the K_i value the stronger the force required to pull out the compound from the receptor binding pocket (Fig. 4C and Figure S7). Additionally, although the force profiles of the ligand induced unbinding event reported in Figures 4C and S7 are similar for each couple of analogous compounds, they reveal a consistently lower dissociative force peak from the receptor for the **3** series with respect to the alternative **2** derivatives. As an example, the peak force required to unbind ligand (2*S*,6*R*)-**3a** (Fig. 4C) is approximately 725 pN, while its cyclohexane analog (1*R*,3*S*)-**2a** (NR_2 = NHBn) requires a stronger force of ~800 pN to fully unbind, in line with its experimental K_i-value.

2.5. Inhibition of tumor cell growth

Due to their promising *in vitro* properties the effect of the stereoisomeric benzylamines **3a** and cyclohexylmethylamines **3b** on tumor cell growth was investigated. The antiproliferative effects of amines **3a** and **3b** was evaluated with the androgen negative human prostate cancer cell line DU145 [59]. The principle of the assay is as follows: in a 96-well plate, DU145 tumor cells were seeded and incubated. After 24 h, the cells were treated with the test compounds in a concentration of 10 μM. After an incubation period of 72 h, survival/proliferation of the DU145 tumor cells was recorded by staining with *Sulforhodamine B* [60].

The stereoisomeric benzylamines **3a** and cyclohexylmethylamines **3b** revealed considerable inhibition of the DU145 tumor cell growth (Fig. 5), which was comparable to that seen for reference σ_1 antagonists NE-100 (ca. 65% growth inhibition) and recently described cyclohexylmethylamines (1*R*,3*S*)-**2a** (NR_2 = NHBn, ca. 71% growth inhibition) and (1*S*,3*R*)-**2a** (NR_2 = NHBn, ca. 67% growth inhibition) tested under the same conditions [42]. The cyclohexylmethylamines **3b** exhibited stronger antiproliferative activity than the corresponding benzylamines **3a**, which correlates nicely with the slightly higher σ_1 (≈2-fold) and considerably higher σ_2 receptor affinity (≈10-fold) of the cyclohexylmethylamines **3b**. However, as demonstrated for the receptor affinity, the antiproliferative activity of the enantiomers is quite similar. In particular, the cyclohexylmethylamines **3b** are regarded as promising candidates for treatment of human tumors.

2.6. In vivo activity of benzylamine and cyclohexylmethylamine enantiomers 3a and 3b in a mechanical allodynia assay

The enantiomeric benzylamines (2*R*,6*S*)-**3a** and (2*S*,6*R*)-**3a** as well as the cyclohexylmethylamines (2*R*,6*S*)-**3b** and (2*S*,6*R*)-**3b** were selected for *in vivo* studies due to their high σ_1 affinity and

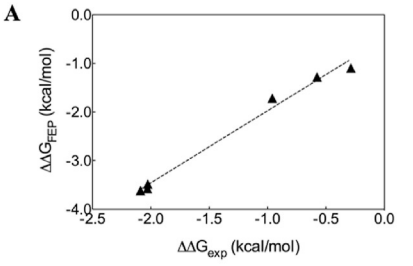

B

2-derivative	3-derivative	-NR_2	$\Delta\Delta G_{FEP}$ (kcal/mol)
(1*R*,3*S*)-**2a**	(2*S*,6*R*)-**3a**	NHBn	-1.30
(1*R*,3*S*)-**2c**	(2*S*,6*R*)-**3c**	$NH(CH_2)_4Ph$	-1.72
(1*R*,3*S*)-**2d**	(2*S*,6*R*)-**3d**	$N(CH_3)_2$	-3.62
(1*R*,3*S*)-**2e**	(2*S*,6*R*)-**3e**		-3.58
(1*R*,3*S*)-**2f**	(2*S*,6*R*)-**3f**		-1.10
(1*R*,3*S*)-**2g**	(2*S*,6*R*)-**3g**	NH_2	-3.48

Fig. 4. (A) Free energy difference values ($\Delta\Delta G = \Delta G$(**2**-derivative) $- \Delta G$(**3**-derivative)) obtained from FEP simulations ($\Delta\Delta G_{FEP}$) and their correlation with the relevant values ($\Delta\Delta G_{exp}$) extrapolated from the experimentally determined K_i values (see Table 3) using the relationship $\Delta G_{exp} = -RT\ln(1/K_i)$. (B) Table with the calculated $\Delta\Delta G_{FEP}$ obtained from the FEP simulations. (C) (top panel) Comparison of the steered molecular dynamics (SMD) force profile for (2*S*,6*R*)-**3a** (cornflower blue) and (1*R*,3*S*)-**2a** (NR_2 = NHBn, purple); (bottom panel) representative snapshots extracted from the SMD simulation of the σ_1 unbinding event of (2*S*,6*R*)-**3a**.

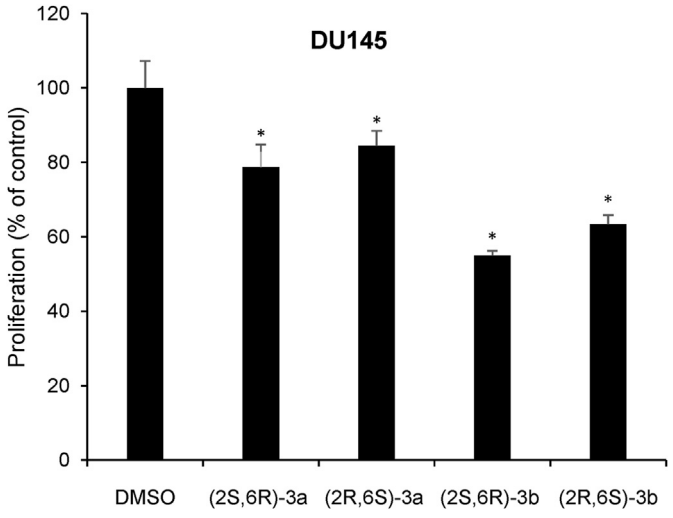

Fig. 5. Growth inhibition of human prostate tumor cells DU145 by stereoisomeric benzylamines **3a** and cyclohexylmethylamines **3b** (10 μM) compared to DMSO.

Table 4
Antiallodynic activity of **3a** and **3b** enantiomers (40 mg/kg body weight).

compd.	% analgesia ±SEM
(2*R*,6*S*)-**3a**	55 ± 1.6
(2*S*,6*R*)-**3a**	21 ± 12.5
(2*R*,6*S*)-**3b**	53 ± 3.7
(2*S*,6*R*)-**3b**	67 ± 5.3
S1RA	97 ± 2.3

promising selectivity over related receptors, transporters and CYP enzymes. It has been shown that σ_1 receptor antagonists can be used for the treatment of allodynia. Therefore, the effects of the four compounds on mechanical allodynia in the capsaicin assay [24,25] were investigated. In this assay, mechanical allodynia was induced by intraplantar administration of capsaicin in mice. 30 min before capsaicin administration, 40 mg/kg body weight of the test compounds were administered subcutaneously and the mechanical allodynia was analyzed with an electronic von Frey device 15 min after capsaicin administration.

At a concentration of 40 mg/kg body weight, the (tetrahydropyranyl)ethanamines **3a** and **3b** showed considerable analgesic activity indicating that the four compounds behave as σ_1 receptor antagonists (Table 4). The cyclohexylmethylamine (2*S*,6*R*)-**3b** revealed higher antiallodynic activity than the analogous benzylamine (2*S*,6*R*)-**3a**, which correlates nicely with its higher σ_1 and σ_2 affinity. Whereas the antiallodynic activity of the benzylamine enantiomers is quite different, the antiallodynic activity of the corresponding cyclohexylmethylamine enantiomers is very similar. Altogether, the (2*S*,6*R*)-configured cyclohexylmethylamine (2*S*,6*R*)-**3b** exhibited the highest σ_1 affinity ($K_i(\sigma_1)$ = 0.95 nM) and the highest analgesic activity (67%) in this series of compounds. Although the analgesic activity of S1RA (see introduction) is higher, the analgesic activity of the tetrahydropyran derivatives **3a** and **3b** prove their σ_1 antagonistic activity.

3. Conclusion

Antagonists at the σ_1 receptor have promising analgesic and antiproliferative activity on tumor cells. Racemic 1,3-dioxane **1** showed high σ_1 affinity (K_i = 19 nM) and high antiallodynic activity *in vivo* in the mouse capsaicin assay [40]. The analogous cyclohexane derivatives (1*R*,3*S*)-**2a** and (1*S*,3*R*)-**2a** (NR_2 = NHBn) exhibited also very high σ_1 receptor affinity (K_i = 0.6 nM, K_i = 1.3 nM) and antiproliferative activity on prostate tumor cells DU145 [42]. In this project, tetrahydropyran derivatives **3** with the same substitution pattern were designed to improve the hydrolytic stability of acetalic 1,3-dioxanes **1** and to increase the polarity of cyclohexanes **2**.

The key step of the synthesis of enantiomerically pure tetrahydropyrans **3** was the kinetic resolution of racemic alcohol (±)-**5** using an enantioselective acetylation with isopropenyl acetate catalyzed by Amano lipase PS-IM. The alcohols (*S*)-**5** and (*R*)-**5**, which were obtained in 99.4% ee and 98.8% ee, respectively, were transformed into seven pairs of enantiomeric amines **3a**-**g** differing in the substituents of the amino moiety. The absolute configuration was determined by CD spectroscopy.

In receptor binding studies with the radioligand [^{3}H](+)-pentazocine, the enantiomeric benzylamines (2*R*,6*S*)-**3a** and (2*S*,6*R*)-**3a** as well as the cyclohexylmethylamines (2*R*,6*S*)-**3b** and (2*S*,6*R*)-**3b** showed low nanomolar up to subnanomolar ((2*S*,6*R*)-**3b**, K_i = 0.95 nM) σ_1 receptor affinity. Despite the very high σ_1 receptor affinity, the eudismic ratio of both pairs of enantiomers was rather low (2.5−3.3). All four compounds exhibited high selectivity over related (e.g. σ_2 receptor, PCP binding site) and further targets (e.g. 5-HT, noradrenalin, opioid receptors, neurotransmitter transporter, CYP enzymes).

The studies performed *in silico via* three different computational techniques (MD, FEP and SMD) yielded interesting insights on the interaction between the receptors and the two different series of ligands. Specifically, MD simulations revealed that the new tetrahydropyran compounds **3** and their previous, cyclohexane-based generation **2** molecules adopt the same binding mode within the σ_1 binding site. Remarkably, according to the MD evidences the additional O-atom of the tetrahydropyrans **3** appears to be dispensable for receptor affinity, as no particular interactions of the O-atom with the target protein were detected. FEP calculations were able to capture the decreased affinity of tetrahydropyrans **3** for the target receptor with respect to their cyclohexane counterparts **2**, yielding free binding energy difference values in excellent match with those obtained from the corresponding experimental data. Finally, FEP data were further confirmed by SMD simulations, according to which weaker forces are consistently required to fully unbind tetrahydropyrans **3** from the protein binding site with respect to the alternative cyclohexane derivatives **2**, again in line with the trend exhibited by the corresponding experimental K_i-value.

The most potent σ_1 receptor ligands (2*R*,6*S*)-**3a**,**b** and (2*S*,6*R*)-**3a**,**b** showed promising antiproliferative activity on the androgen negative human prostate cancer cell line DU145. This effect correlates well with the antiproliferative activity of the enantiomeric cyclohexanes (1*R*,3*S*)-**2a** and (1*S*,3*R*)-**2a**. These potent σ_1 receptor ligands (2*R*,6*S*)-**3a**,**b** and (2*S*,6*R*)-**3a**,**b** were also active in the capsaicin assay, an animal model for mechanical allodynia. The most potent σ_1 receptor ligand (2*S*,6*R*)-**3b** (K_i = 0.95 nM) displayed the highest antiallodynic activity in this assay. The analgesic activity in the capsaicin assay confirms the antagonistic activity of the tetrahydropyrans **3**.

It can be concluded that one O-atom in the six-membered ring of **3** maintains the biological activity of the potent 1,3-dioxane and cyclohexane derivatives **1** and **2**. Although this O-atom is not essential for high σ_1 receptor binding, it is essential to increase the polarity and thus the pharmacokinetic properties of the tetrahydropyrans **3**. The instability of the acetalic 1,3-dioxanes **1** against acid (stomach) was overcome by removal of one O-atom. Regarding the lipophilicity, the tetrahydropyrans ($clogD_{7.4}$ (**3a**) = 2.05)

represent a good compromise between 1,3-dioxanes **1** and cyclohexanes **2**. The favorable pharmacokinetics of the tetrahydropyrans **3** was demonstrated by their activity in the capsaicin assay, proving the *in vivo* activity and the penetration of the blood-brain-barrier.

4. Experimental

4.1. Chemistry, general

Unless otherwise noted, moisture sensitive reactions were conducted under dry nitrogen. CH_2Cl_2 was distilled over CaH_2. THF was distilled over sodium/benzophenone. Et_2O and toluene were dried over molecular sieve 0.4 Å. Thin layer chromatography (tlc): Silica gel 60 F254 plates (Merck). Flash chromatography (fc): Silica gel 60, 40–64 μm (Merck); parentheses include: diameter of the column (d), length of the stationary phase, fraction size (V), eluent. Melting point: Melting point apparatus Mettler Toledo MP50 Melting Point System, uncorrected. MS: microOTOF-Q II (Bruker Daltonics); APCI, atmospheric pressure chemical ionization. IR: FT-IR spectrophotometer MIRacle 10 (Shimadzu) equipped with ATR technique. Circular dichroism spectroscopy: JASCO J-600 spectropolarimeter (Jasco, Groβ-Umstadt), 0.1 cm dell, solvent CH3CN. Nuclear magnetic resonance (NMR) spectra were recorded on Agilent 600-MR (600 MHz for ^{1}H, 151 MHz for ^{13}C) or Agilent 400-MR spectrometer (400 MHz for ^{1}H, 101 MHz for ^{13}C); δ in ppm related to tetramethylsilane and measured referring to $CHCl_3$ (δ = 7.26 ppm (^{1}H NMR) and δ = 77.2 ppm (^{13}C NMR)), CHD_2OD (δ = 3.31 ppm (^{1}H NMR) and δ = 49.0 ppm (^{13}C NMR)) and DMSO-d_6 (δ = 2.54 ppm (^{1}H NMR) and δ = 39.5 ppm (^{13}C NMR)); coupling constants are given with 0.5 Hz resolution; the assignments of ^{13}C and ^{1}H NMR signals were supported by 2-D NMR techniques where necessary.

4.2. HPLC equipment and methods

HPLC method 1 to determine the purity of compounds: Pump: L-7100, degasser: L-7614, autosampler: L-7200, UV detector: L-7400, interface: D-7000, data transfer: D-line, data acquisition: HSM-Software (all from LaChrom, Merck Hitachi); Equipment 2: Pump: LPG-3400SD, degasser: DG-1210, autosampler: ACC-3000T, UV-detector: VWD-3400RS, interface: DIONEX UltiMate 3000, data acquisition: Chromeleon 7 (Thermo Fisher Scientific); column: LiChropher® 60 RP-select B (5 μm), LiChroCART® 250-4 mm cartridge; flow rate: 1.0 mL/min; injection volume: 5.0 μL; detection at λ = 210 nm; solvents: A: demineralized water with 0.05% (V/V) trifluoroacetic acid, B: acetonitrile with 0.05% (V/V) trifluoroacetic acid; gradient elution (% A): 0–4 min: 90%; 4–29 min: gradient from 90% to 0%; 29–31 min: 0%; 31–31.5min: gradient from 0% to 90%; 31.5–40 min: 90%. The purity of all test compounds is greater than 95%.

4.3. Synthetic procedures

4.3.1. Ethyl 5-hydroxy-5-phenylpentanoate ((±)-5)

The ketone **4** (10.91 g, 49.52 mmol) was dissolved in ethanol (dried over molecular sieves 3 Å, 80 mL) and $NaBH_4$ (562 mg, 14.86 mmol) was added under N_2. The solution was stirred at room temperature for 6 h. Under ice cooling, 2 M HCl was added until the mixture was neutral. Then, brine (75 mL) was added and the mixture was extracted with CH_2Cl_2 (3 x 40 mL). The combined organic layers were dried (Na_2SO_4), the solvent was evaporated in vacuo and the residue was purified by flash column chromatography (Ø 8 cm, h 15 cm, 65 mL, cyclohexane:ethyl acetate = 4:1, R_f = 0.27). Colorless oil, yield 7.41 g (67%). Purity (HPLC method 1): 97.7% (t_R = 17.1 min). $C_{13}H_{18}O_3$ (222.3 g/mol). MS (ESI): *m/z* = 467 (2 M + Na^+), 245 (M + Na^+), 205 (M − OH). IR: $\tilde{\nu}$ (cm^{-1}) = 3438 (O–H broad), 2935 (C–H), 1731 (C=O), 761, 700 (C-H_{arom}). ^{1}H NMR ($CDCl_3$): δ (ppm) = 1.16 (t, *J* = 7.1 Hz, 3H, OCH_2CH_3), 1.50–1.78 (m, 4H, $CH_2CH_2CO_2R$), 1.94 (d, *J* = 3.4 Hz, 1H, O*H*), 2.25 (td, J = 7.0/1.6 Hz, 2H, PhCHOHCH_2), 4.03 (q, *J* = 7.1 Hz, 2H, OCH_2CH_3), 4.59–4.62 (m, 1H, PhC*H*OH), 7.18–7.29 (m, 5H, arom). ^{13}C NMR ($CDCl_3$): δ (ppm) = 14.2 (1C, OCH_2CH_3), 21.2 (1C, $CH_2CH_2CH_2$), 34.0 (1C, CH_2COOR), 38.3 (1C, PhCHOHCH_2), 60.3 (1C, OCH_2CH_3), 74.1 (1C, PhCHOH), 125.8 (2C, C-2, C-6 arom), 127.6 (1C, C-4 arom), 128.5 (2C, C-3, C-5 arom), 144.5 (1C, C-1 arom), 173.6 (1C, CO_2R).

4.3.2. Ethyl 5-acetoxy-5-phenylpentanoate ((±)-6)

Under N_2 acetic anhydride (0.14 mL, 1.53 mmol) and NEt_3 (0.21 mL, 1.53 mmol) were added to a solution of the alcohol (±)-**5** (170 mg, 0.76 mmol) in $THF_{(abs)}$ (8 mL) and the solution was heated to reflux for 29 h. Additional acetic anhydride was added after 3 h (0.28 mL, 3.06 mmol) and 21 h (0.28 mL, 3.06 mmol). The mixture was transferred to a separating funnel. A saturated solution of $NaHCO_3$ (15 mL) and NaCl were added and the mixture was extracted with CH_2Cl_2 (3 x 10 mL). The organic layer was dried (Na_2SO_4), filtered and the solvent was evaporated in vacuo. The residue was purified by flash column chromatography (Ø 3.5 cm, h 13 cm, 10 mL, cyclohexane:ethyl acetate = 4:1, R_f = 0.55). Colorless oil, yield 80 mg (40%). Purity (HPLC method 1): 95.9% (t_R = 20.4 min). $C_{15}H_{20}O_4$ (264.3 g/mol). MS (ESI): *m/z* = 287 (M + Na^+). IR: $\tilde{\nu}$ (cm-1) = 2942 (C–H), 1730 (C=O), 760, 699 (C-H_{arom}). ^{1}H NMR ($CDCl_3$): δ (ppm) = 1.24 (t, *J* = 7.1 Hz, 3H, OCH_2CH_3), 1.51–1.98 (m, 4H, $CH_2CH_2CH_2CO_2R$), 2.07 (s, 3H, $OCOCH_3$), 2.31 (t, *J* = 7.4 Hz, 2H, CH_2CO_2R), 4.11 (q, *J* = 7.1 Hz, 2H, OCH_2CH_3), 5.71–5.75 (dd, J = 7.7/6.0 Hz, 1H, PhC*H*OH), 7.27–7.36 (m, 5H, arom).

4.3.3. Ethyl (S)-5-hydroxy-5-phenylpentanoate ((S)-5) and ethyl (R)-5-acetoxy-5-phenylpentanoate ((R)-6)

A solution of the racemic alcohol *rac*-**5** (7.59 g, 34 mmol) in TBME (500 mL) was added to Amano lipase PS-IM (7.54 g). Then isopropenyl acetate (18.6 mL, 171 mmol) was added and the mixture was stirred for 6 d. To remove the lipase, the mixture was filtered, the filter was washed with TBME and the solvent was removed in vacuo. The ratio of (*R*)-**6**: (*S*)-**6** was 55 : 45 (HPLC method B (Supporting Information)), t_R(**6**) = 15.8 min, t_R(**5**) = 6.2 min). The two products were separated and purified by flash column chromatography (Ø 8 cm, h 17 cm, 65 mL, cyclohexane:ethyl acetate = 4:1, R_f = 0.55 for (*R*)-**6**, R_f = 0.27 for (*S*)-**5**).

(*S*)-**5:** Colorless oil, yield 3.10 g (41%). Purity (HPLC method 1): 96.1% (t_R = 16.9 min). Enantiomeric purity (HPLC method A1 (Supporting Information)): 99.68:0.32 (t_R = 21.9 min). Specific rotation: $[\alpha]_D^{20} = -29.4$ (c = 1.40; CH_2Cl_2). For further analytical data see (±)-**5**.

(*R*)-**6:** Colorless oil, yield 4.45 g (49%). Purity (HPLC method 1): 99.7% (t_R = 20.1 min). Further analytical data see (±)-**6**.

4.3.4. Ethyl (R)-5-hydroxy-5-phenylpentanoate ((R)-5)

K_2CO_3 (585 mg, 4.23 mmol) was added to a solution of enantiomerically enriched acetate (*R*)-**5** (4.45 g, 16.85 mmol) in ethanol (dried over molecular sieves 3 Å, 70 mL). The mixture was stirred at room temperature for 15.5 h. Then it was neutralized with 2 M HCl. H_2O (75 mL) was added and the aqueous layer was extracted with CH_2Cl_2 (4 x 25 mL). The combined organic layers were dried (Na_2SO_4), filtered and the solvent was removed in vacuo. The crude product was purified by flash column chromatography (Ø 8 cm, h 16 cm, 65 mL, cyclohexane:ethyl acetate = 4:1). Colorless oil, yield 3.07 g (82%). Purity (HPLC method 1): 99.4% (t_R = 16.9 min). Enantiomeric purity (HPLC method A1 (Supporting Information)):

89.05:10.95. To a mixture of the resulting alcohol (*R*)-**5** (3.07 g, 13.8 mmol) and Amano lipase PS-IM (3.05 g) in TBME (200 mL), isopropenyl acetate (7.5 mL, 69.13 mmol) was added to start the reaction. The mixture was stirred for 3.5 d. The lipase was filtered off and the residue was washed with TBME. The combined TBME layers were dried (Na_2SO_4), again filtered and the solvent was evaporated in vacuo. The ratio of acetate and alcohol was 82:18 (HPLC method B (Supporting Information)). The residue was purified by flash column chromatography (Ø 8 cm, h 15 cm, 65 mL, cyclohexane: ethyl acetate = 4:1). Colorless oil, yield 3.04 g (82%). Purity (HPLC method 1): 99.9% (t_R = 20.1 min). K_2CO_3 (397 mg, 2.87 mmol) was added to a solution of acetate (*R*)-**6** (3.04 g, 11.49 mmol) in ethanol (dried over molecular sieves 3 Å, 50 mL). After stirring for 22 h, the solution was neutralized with 2 M HCl, H_2O (75 mL) was added and the mixture was extracted with CH_2Cl_2 (4 x 25 mL). The combined organic layers were dried (Na_2SO_4), filtered and the solvent was removed in vacuo. The crude product was purified by flash column chromatography (Ø 6.5 cm, h 16 cm, 65 mL, cyclohexane:ethyl acetate = 4:1). (*R*)-**5** Colorless oil, yield 2.23 g (88%). Purity (HPLC method 1): 99.4% (t_R = 17.0 min). Enantiomeric purity (HPLC method A1 (Supporting Information)): 99.42:0.58 (t_R = 18.8 min). Specific rotation: $[\alpha]_D^{20} = +30.0$ (c = 1.40; CH_2Cl_2). Further analytical data see (±)-**5**.

4.3.5. 6-Phenyltetrahydropyran-2-one ((±)-7)

Under ice cooling trifluoroacetic acid (0.05 mL) was added to a solution of (±)-**5** (329 mg, 1.48 mmol) in CH_2Cl_2 (50 mL) and the mixture was stirred for 24 h at room temperature. Then the mixture was transferred into a separating funnel and the organic layer was washed with a saturated solution of $NaHCO_3$ and H_2O. Afterwards the organic layer was dried (Na_2SO_4), filtered and the solvent was evaporated in vacuo. The crude product was purified by flash column chromatography (Ø 3.5 cm, h 14 cm, 10 mL, cyclohexane:ethyl acetate = 5:1, R_f = 0.16). Colorless solid, mp 99 °C, yield 187 mg (72%). Purity (HPLC method 1): 94.3% (t_R = 15.8 min). $C_{11}H_{12}O_2$ (176.2 g/mol). MS (ESI): *m*/*z* = 194 ($M + NH_4^+$), 177 ($M + H^+$). IR: $\tilde{\nu}$ (cm^{-1}) = 2953 (C—H), 1716 (C═O), 757, 702 (C-H_{arom}). ^{1}H NMR ($CDCl_3$): δ (ppm) = 1.82—2.02 (m, 3H, pyran), 2.14—2.21 (m, 1H, pyran), 2.58 (dt, J = 17.8/7.7 Hz, 1H, OCOC*H*$_2$), 2.72 (dt, J = 17.8/6.5 Hz, 1H, OCOC*H*$_2$), 5.36 (dd, J = 10.5/3.5 Hz, 1H, PhC*H*), 7.30—7.40 (m, 5H, arom).

4.3.6. (S)-6-Phenyltetrahydropyran-2-one ((S)-7)

As described for *rac*-**7**, a solution of (*S*)-**5** (8.61 g, 38.7 mmol) and trifluoroacetic acid (15 drops) in CH_2Cl_2 (90 mL) was stirred for 29 h. After 7 h and 24 h additional trifluoroacetic acid (15 drops each) was added. The product was purified twice by flash column chromatography (1. Ø 8 cm, h 16 cm, 65 mL, cyclohexane:ethyl acetate = 5:1, R_f = 0.16, 2. Ø 6.5 cm, h 15 cm, 65 mL, cyclohexane:ethyl acetate = 2:1, R_f = 0.32). Colorless solid, yield 2.47 g (36%). Purity (HPLC method 1): 92.2% (t_R = 15.4 min). Specific rotation: $[\alpha]_D^{20} = -23.0$ (c = 1.05; CH_2Cl_2). Further analytical data see (±)-**7**.

4.3.7. (R)-6-Phenyltetrahydropyran-2-one ((R)-7)

According to (±)-**7**, a solution of (*R*)-**5** (8.77 g, 39.4 mmol) and trifluoroacetic acid (30 drops) in CH_2Cl_2 (110 mL) was stirred for 34 h. The crude product was purified by flash column chromatography twice (1. Ø 8 cm, h 16 cm, 65 mL, cyclohexane:ethyl acetate = 6:1, R_f = 0.10, 2. Ø 6.5 cm, h 16 cm, 65 mL, cyclohexane:ethyl acetate = 2:1, R_f = 0.32). Colorless solid, yield 2.07 g (30%). Purity (HPLC method 1): 92.1% (t_R = 15.6 min). Specific rotation: $[\alpha]_D^{20} = +23.0$ (c = 1.05; CH_2Cl_2). Further analytical data see (±)-**7**.

4.3.8. 6-Phenyltetrahydropyran-2-ol ((±)-8)

Under N_2 the lactone (±)-**7** (76 mg, 0.43 mmol) was dissolved in CH_2Cl_2 (10 mL) and the solution was cooled to −78 °C. A 1 M solution of DIBAL in toluene (0.54 mL, 0.54 mmol) was added dropwise and the mixture was stirred for 1 h at −78 °C. A saturated solution of $NaHCO_3$ and CH_2Cl_2 were added. After warming up to room temperature the reaction mixture was washed with a mixture of 10% HCl/saturated NH_4Cl solution (1/1.5). The organic layer was dried ($NaSO_4$), filtered and concentrated in vacuo. The residue was purified by flash column chromatography (Ø 3 cm, h 14 cm, 10 mL, cyclohexane:ethyl acetate = 4:1, R_f = 0.33). Colorless solid, mp 62 °C, yield 66 mg (86%). Purity (HPLC method 1): 98.3% (t_R = 14.9 min). $C_{11}H_{14}O_2$ (178.2 g/mol). MS (ESI): *m*/*z* = 177 ($M - H^+$). IR: $\tilde{\nu}$ (cm^{-1}) = 3350 (O—H), 2951 (C—H), 760, 697 (C-H_{arom}). ^{1}H NMR ($CDCl_3$): δ (ppm) = 1.25—2.18 (m, 6H, pyran), 2.61—2.62 (m, 0.5H, O*H*), 3.03 (d, *J* = 5.8 Hz, 0.5H, O*H*), 4.50 (dd, J = 11.2/2.2 Hz, 0.5H, PhC*H*), 4.90 (ddd, J = 9.4/5.8/1.9 Hz, 0.5H, C*H*OH), 5.03 (dd, J = 11.5/2.3 Hz, 0.5H, PhC*H*), 5.47 (m, 0.5H,C*H*OH), 7.24—7.41 (m, 5H, arom). The ratio of the two diastereomers is 52:48.

4.3.9. (6S)-6-phenyltetrahydropyran-2-ol ((S)-8)

As described for (±)-**8**, to a solution of (*S*)-**7** (980 mg, 5.56 mmol) in CH_2Cl_2 (60 mL), a 1.2 M solution of DIBAL in toluene (5.8 mL, 6.95 mmol) was added and the mixture was stirred for 2 h at −78 °C. The residue was purified by flash column chromatography (Ø 4 cm, h 17 cm, 30 mL, cyclohexane:ethyl acetate = 4:1). Colorless solid, yield 944 mg (95%). Purity (HPLC method 1): 99.6% (t_R = 14.6 min). Specific rotation: $[\alpha]_D^{20}$ = - 29.7 (c = 1.53; CH_2Cl_2). Further analytical data see (±)-**8**.

4.3.10. (6R)-6-phenyltetrahydropyran-2-ol ((R)-8)

As described for (±)-**8**, a solution of (*R*)-**7** (3.39 g, 19.22 mmol) in CH_2Cl_2 (140 mL) was treated with a 1.2 M solution of DIBAL in toluene (20.0 mL, 24 mmol) and the mixture was stirred for 2 h at −78 °C. The product was purified by flash column chromatography (Ø 6.5 cm, h 15 cm, 65 mL, cyclohexane:ethyl acetate = 4:1). Colorless solid, yield 3.29 g (96%). Purity (HPLC method 1): 98.7% (t_R = 14.6 min). Specific rotation: $[\alpha]_D^{20} = +29.7$ (c = 1.53; CH_2Cl_2). Further analytical data see (±)-**8**.

4.3.11. Methyl trans-7-hydroxy-7-phenylhept-2-enoate ((±)-9)

A solution of $Ph_3P{=}CHCO_2CH_3$ (437 mg, 1.31 mmol) in THF was added to a solution of lactol (±)-**8** (156 mg, 0.87 mmol) in THF (30 mL). The mixture was heated to reflux for 5.5 h. The solvent was evaporated in vacuo and the residue was purified by flash column chromatography (Ø 4 cm, h 18 cm, 10 mL, cyclohexane:ethyl acetate = 5:1, R_f = 0.21). Colorless oil, yield 55 mg (27%). Purity (HPLC method 1): 98.8% (t_R = 17.8 min). $C_{14}H_{18}O_3$ (234.3 g/mol). MS (EI): *m*/*z* = 235 ($M + H^+$), 217 (M − OH), 157 (M − Ph), 77 (Ph). IR: $\tilde{\nu}$ (cm^{-1}) = 3447 (O—H broad), 2947 (C—H), 1720 (C═O), 761, 700 (C-H_{arom}). ^{1}H NMR ($CDCl_3$): δ (ppm) = 1.40—1.85 (m, 4H, CHOHC*H*$_2$C*H*$_2$), 1.86 (d, *J* = 3.2 Hz, 1H, O*H*), 2.22 (qd, J = 7.2/1.5 Hz, 2H, C*H*$_2$CH═CH), 3.71 (s, 3H, OC*H*$_3$), 4.66—4.70 (m, 1H, C*H*OH), 5.80 (dt, J = 15.7/1.6 Hz, 1H, CH═C*H*CO_2R), 6.93 (dt, J = 15.7/7.0 Hz, 1H, C*H*═CHCO_2R), 7.26—7.38 (m, 5H, arom).

4.3.12. Methyl trans-(7S)-7-hydroxy-7-phenylhept-2-enoate ((S)-9)

As described for (±)-**9**, (*S*)-**8** (3.12 g, 17.50 mmol) was reacted with $Ph_3P{=}CHCO_2CH_3$ (8.72 g, 26.08 mmol) in THF (150 mL). The mixture was heated to reflux for 20 h. The product was purified by flash column chromatography (Ø 8 cm, h 15 cm, 65 mL, cyclohexane:ethyl acetate = 5:1). Colorless oil, yield 2.57 g (63%). Purity

(HPLC method 1): 97.9% (t_R = 18.0 min). Specific rotation: $[\alpha]_D^{20} = -21.4$ (c = 1.20; CH_2Cl_2). Further analytical data see (±)-**9**.

4.3.13. Methyl trans-(7R)-7-hydroxy-7-phenylhept-2-enoate ((R)-9)

As described for (±)-**9**, a solution of (*R*)-**8** (3.21 g, 18.04 mmol) and $Ph_3P{=}CHCO_2CH_3$ (9.02 g, 26.98 mmol) in THF (150 mL) was heated to reflux for 19 h. The residue was purified by flash column chromatography (Ø 8 cm, h 15 cm, 65 mL, cyclohexane:ethyl acetate = 5:1). Pale yellow oil, yield 2.11 g (50%). Purity (HPLC method 1): 98.2% (t_R = 18.0 min). Specific rotation: $[\alpha]_D^{20} = +24.6$ (c = 1.20; CH_2Cl_2). Further analytical data see (±)-**9**.

4.3.14. Methyl 2-[(2RS,6SR)-6-phenyltetrahydropyran-2-yl]acetate ((±)-10)

The α,β-unsaturated ester (±)-**9** (306 mg, 1.31 mmol) was dissolved in THF (12 mL) and a 1 M solution of KO^{t}Bu (0.65 mL, 0.65 mmol) was added. The mixture was stirred under N_2 for 23 h at room temperature. Then H_2O (20 mL) was added and the mixture was extracted with CH_2Cl_2 (4 x 10 mL). To improve the separation of the layers, NaCl, H_2O and CH_2Cl_2 were added. The combined organic layers were dried (Na_2SO_4), filtered, concentrated in vacuo and the residue was purified by flash column chromatography (Ø 3.5 cm, h 17 cm, 10 mL, cyclohexane:ethyl acetate = 7:1, R_f = 0.5). Colorless oil, yield 134 mg (44%). Purity (HPLC method 1): 95.9% (t_R = 20.5 min). $C_{14}H_{18}O_3$ (234.3 g/mol). MS (EI): *m/z* = 235 ($M + H^+$), 234 (M). IR: $\tilde{\nu}$ (cm^{-1}) = 2936, 2859 (C−H), 1737 (C=O), 1073, 1042 (C−O), 749, 698 (C-H_{arom}). ^{1}H NMR ($CDCl_3$): δ (ppm) = 1.30−1.57 (m, 2H, pyran), 1.66−1.78 (m, 2H, pyran), 1.83−1.89 (m, 1H, pyran), 1.93−1.99 (m, 1H, pyran), 2.49 (dd, J = 15.1/6.0 Hz, 1H, C*H*$_2$CO$_2$R), 2.67 (dd, J = 15.2/7.1 Hz, 1H, C*H*$_2$CO$_2$R), 3.68 (s, 3H, OC*H*$_3$), 3.95−4.02 (m, 1H, OC*H*R$_2$), 4.41 (dd, J = 11.3/2.2 Hz, 1H, PhC*H*), 7.22−7.39 (m, 5H, arom). NOE: Irradiation at 3.98 ppm (OC*H*R$_2$): δ (ppm) = 1.66−1.78 (pyran), 2.49 (C*H*$_2$CO$_2$R), 2.67 (C*H*$_2$CO$_2$R), 4.41 (PhC*H*). Irradiation at 4.41 ppm (PhC*H*): δ (ppm) = 1.83−1.89 (pyran), 3.95−4.02 (OC*H*R$_2$), 7.22−7.39 (arom).

4.3.15. Methyl 2-[(2R,6S)-6-phenyltetrahydropyran-2-yl]acetate ((2R,6S)-10)

Under N_2 the α,β-unsaturated ester (*S*)-**9** (2.54 g, 10.84 mmol) was dissolved in THF (140 mL). Under ice cooling a 1 M solution of KO^{t}Bu in THF (2.7 mL, 2.7 mmol) was added and the mixture was stirred for 2.5 h at room temperature. Saturated solutions of NH_4Cl and 2 M HCl were added and the mixture was concentrated in vacuo. H_2O was added and the aqueous layer was extracted with CH_2Cl_2 (4 x 30 mL). The combined organic layers were dried (Na_2SO_4), filtered, the solvent was removed in vacuo and the residue was purified by flash column chromatography (Ø 6.5 cm, h 15 cm, 65 mL, cyclohexane:ethyl acetate = 10:1, R_f = 0.3). Colorless oil, yield 1.63 g (64%). Purity (HPLC method 1): 95.8% (t_R = 20.1 min). Specific rotation: $[\alpha]_D^{20} = -63.6$ (c = 1.50; CH_2Cl_2). Further analytical data see (±)-**10**.

4.3.16. Methyl 2-[(2S,6R)-6-phenyltetrahydropyran-2-yl]acetate ((2S,6R)-10)

As described for (2*R*,6*S*)-**10**, (*R*)-**9** (2.06 g, 8.79 mmol) was dissolved in THF (100 mL) and reacted with a 1 M solution of KO^{t}Bu in THF (2.20 mL, 2.20 mmol). The residue was purified by flash column chromatography (6.5 cm, h 16 cm, 65 mL, cyclohexane:ethyl acetate = 10:1). Colorless oil, yield 1.34 g (65%). Purity (HPLC method 1): 95.9% (t_R = 20.1 min). Specific rotation: $[\alpha]_D^{20} = +59.4$ (c = 1.50; CH_2Cl_2). Further analytical data see (±)-**10**.

4.3.17. 2-[(2RS,6SR)-6-phenyltetrahydropyran-2-yl]ethan-1-ol ((±)-11)

Under N_2 the racemic ester (±)-**10** (403 mg, 1.72 mmol) was dissolved in THF (26 mL). Under ice cooling, a 1 M solution of $LiAlH_4$ in THF (1.80 mL, 1.80 mmol) was added dropwise and the mixture was stirred at 0 °C. After 30 min the ice bath was removed and the mixture was stirred for 2 h at room temperature. H_2O was added under ice cooling until the gas formation stopped. The mixture was heated to reflux for 30 min, filtered and the filter was washed with ethyl acetate. The residue was purified by flash column chromatography (Ø 4 cm, h 15 cm, 10 mL, cyclohexane:ethyl acetate = 4:1, R_f = 0.21). Colorless oil, yield 324 mg (91%). Purity (HPLC method 1): 99.2% (t_R = 17.8 min). $C_{13}H_{18}O_2$ (206.3 g/mol). MS (ESI): *m/z* = 229 ($M + Na^+$), 207 ($M + H^+$). IR: $\tilde{\nu}$ (cm^{-1}) = 3393 (O−H broad), 2934, 2857 (C−H), 1082, 1040 (C−O), 749, 697 (C-H_{arom}). ^{1}H NMR ($CDCl_3$): δ (ppm) = 1.31−1.92 (m, 8H, CH(C*H*$_2$)$_3$CH−C*H*$_2$), 3.67−3.76 (m, 3H, C*H*$_2$OH, OC*H*R$_2$), 4.35 (dd, J = 11.3/2.3 Hz, 1H, PhC*H*), 7.15−7.29 (m, 5H, arom). A signal for the OH-group is not seen in the spectrum.

4.3.18. 2-[(2R,6S)-6-phenyltetrahydropyran-2-yl]ethan-1-ol ((2R,6S)-11)

As described for (±)-**11**, a solution of (2*R*,6*S*)-**10** (342 mg, 1.46 mmol) in THF (20 mL) was reacted with a 1 M solution of $LiAlH_4$ in THF (1.5 mL, 1.5 mmol). The product was purified by flash column chromatography (Ø 3 cm, h 17 cm, 20 mL, cyclohexane:ethyl acetate = 4:1). Colorless oil, yield 271 mg (90%). Purity (HPLC method 1): 95.2% (t_R = 17.4 min). Specific rotation: $[\alpha]_D^{20} = -90.9$ (c = 1.47; CH_2Cl_2). Enantiomeric purity (HPLC method C (Supporting Information)): 99.17:0.83 (t_R = 14.3 min). Further analytical data see (±)-**11**.

4.3.19. 2-[(2S,6R)-6-phenyltetrahydropyran-2-yl]ethan-1-ol ((2S,6R)-11)

As described for (±)-**11**, a 1 M solution of $LiAlH_4$ in THF (5.2 mL, 5.2 mmol) was added to a solution of (2*S*,6*R*)-**10** (1.15 g, 4.91 mmol) in THF (45 mL) and the mixture was stirred under ice cooling for 1.5 h. The product was purified by flash column chromatography (Ø 4 cm, h 18 cm, 20 mL, cyclohexane:ethyl acetate = 4:1). Colorless oil, yield 898 mg (89%). Purity (HPLC method 1): 98.4% (t_R = 17.4 min). Specific rotation: $[\alpha]_D^{20} = +90.3$ (c = 1.47; CH_2Cl_2). Enantiomeric purity (HPLC method C (Supporting Information)): 98.99:1.01 (t_R = 11.4 min). Further analytical data see (±)-**11**.

4.3.20. {2-[(2RS,6SR)-6-Phenyltetrahydropyran-2-yl]ethyl} methanesulfonate ((±)-12)

Under N_2 the alcohol (±)-**11** (79 mg, 0.38 mmol) was dissolved in CH_2Cl_2 (20 mL), NEt_3 (0.16 mL, 1.15 mmol) was added and the solution was stirred for 10 min under ice cooling. Methanesulfonyl chloride (0.04 mL, 0.58 mmol) was added, the ice bath was removed and the reaction mixture was stirred at room temperature overnight. In a separating funnel the mixture was washed with 0.5 M NaOH (2 x) and then with a saturated solution of NH_4Cl (1 x). Afterwards it was dried (Na_2SO_4), filtered, concentrated in vacuo and the residue was purified by flash column chromatography (Ø 2.5 cm, h 15 cm, 10 mL, cyclohexane:ethyl acetate = 4:1, R_f = 0.27). Colorless solid, mp 46 °C, yield 98 mg (90%). Purity (HPLC method 1): 99.1% (t_R = 20.5 min). $C_{14}H_{20}O_4S$ (284.4 g/mol). MS (ESI): *m/z* = 307 ($M + Na^+$). IR: $\tilde{\nu}$ (cm^{-1}) = 2935 (C−H), 1307, 1337, 1177, 1167 (O-mesyl), 737, 700 (C-H_{arom}). ^{1}H NMR ($CDCl_3$): δ (ppm) = 1.31−1.55 (m, 2H, pyran), 1.64−1.76 (m, 2H, pyran), 1.84−2.04 (m, 4H, pyran, C*H*$_2$CH$_2$OMes), 2.94 (s, 3H, OSO$_2$C*H*$_3$), 3.64−3.71 (m, 1H, OC*H*R$_2$), 4.33−4.46 (m, 3H, C*H*$_2$OSO$_2$R, PhC*H*), 7.23−7.38 (m, 5H, arom).

4.3.21. {2-[(2R,6S)-6-Phenyltetrahydropyran-2-yl]ethyl} methanesulfonate ((2R,6S)-12)

As described for (±)-**12**, a solution of the alcohol (2*R*,6*S*)-**11** (256 mg, 1.24 mmol), NEt_3 (0.52 mL, 3.73 mmol) and methanesulfonyl chloride (0.14 mL, 1.86 mmol) in CH_2Cl_2 (40 mL) was stirred overnight. The residue was purified by flash column chromatography (Ø 3 cm, h 14 cm, 10 mL, cyclohexane:ethyl acetate = 4:1). Colorless oil, yield 323 mg (92%). Purity (HPLC method 1): 99.0% (t_R = 20.1 min). Specific rotation: $[\alpha]_D^{20} = -87.3$ (c = 1.62; CH_2Cl_2). Further analytical data see (±)-**12**.

4.3.22. {2-[(2S,6R)-6-Phenyltetrahydropyran-2-yl]ethyl} methanesulfonate ((2S,6R)-12)

As described for (±)-**12**, a solution of the alcohol (2*S*,6*R*)-**11** (1.86 g, 9.04 mmol), NEt_3 (3.8 mL, 27.11 mmol) and methanesulfonyl chloride (1.05 mL, 13.55 mmol) in CH_2Cl_2 (100 mL) was stirred overnight. The crude product was purified by flash column chromatography (Ø 6.5 cm, h 16 cm, 65 mL, cyclohexane:ethyl acetate = 4:1). Colorless oil, yield 2.39 g (93%). Purity (HPLC method 1): 98.4% (t_R = 20.2 min). Specific rotation: $[\alpha]_D^{20} = +87.6$ (c = 1.62; CH_2Cl_2). Further analytical data see (±)-**12**.

4.3.23. N-benzyl-2-[(2RS,6SR)-6-phenyltetrahydropyran-2-yl) ethanamine ((±)-3a)

The mesylate (±)-**12** (60 mg, 0.21 mmol) was dissolved in acetonitrile (15 mL). After adding benzylamine (0.07 mL, 0.63 mmol), the reaction mixture was heated to reflux for 19 h. Then the solvent was evaporated and the residue was taken up in ethyl acetate and extracted with 0.5 M NaOH (2 x). The organic layer was dried (Na_2SO_4), filtered and concentrated in vacuo. The crude product was purified by flash column chromatography (Ø 2 cm, h 16 cm, 10 mL, cyclohexane:ethyl acetate = 7:1 + 1% dimethylethylamine, R_f = 0.13). Pale yellow oil, yield 47 mg (75%). Purity (HPLC method 1): 97.6% (t_R = 18.3 min). $C_{20}H_{25}NO$ (295.4 g/mol). MS (ESI): *m*/*z* = 296 ($M + H^+$). MS (EM, APCI): *m*/*z* = calculated for $C_{20}H_{26}NO$ ($M + H^+$) 296.2009, found 296.2040. IR: $\tilde{\nu}$ (cm^{-1}) = 2933, 2844 (C—H), 1087, 1043 (C—O), 739, 696 (C-H_{arom}). ^1H NMR ($CDCl_3$): δ (ppm) = 1.26—1.96 (m, 8H, CH(C*H*$_2$)$_3$CH—C*H*$_2$), 2.80 (td, J = 6.8/1.2 Hz, 2H, CH_2CH_2NH), 3.57—3.63 (m, 1H, OC*H*R_2), 3.77 (s, 2H, NHC*H*$_2$Ph), 4.36 (dd, J = 11.3/2.1 Hz, 1H, PhC*H*), 7.20—7.35 (m, 10H, arom). A signal for the NH proton is not seen in the spectrum. ^{13}C NMR ($CDCl_3$): δ (ppm) = 24.0, 31.4, 33.6, 36.5 (4C, CH(CH_2)$_3$CH—CH_2), 46.4 (1C, CH_2CH_2NH), 54.0 (1C, NHCH_2Ph), 77.4 (1C, OCHR_2), 79.6 (1C, Ph*C*H), 125.7 (2C, arom), 126.7, 127.0 (2C, C-4 arom), 128.0, 128.2, 128.3 (6C, arom), 140.5, 143.5 (2C, C-1 arom).

4.3.24. N-benzyl-2-[(2R,6S)-6-phenyltetrahydropyran-2-yl] ethanamine ((2R,6S)-3a)

As described for (±)-**3a**, a solution of (2*R*,6*S*)-**12** (175 mg, 0.62 mmol) and benzylamine (0.20 mL, 1.85 mmol) in acetonitrile (17 mL) was heated to reflux for 16 h. The product was purified by flash column chromatography (Ø 3 cm, h 14 cm, 10 mL, cyclohexane:ethyl acetate = 7:1 + 1% dimethylethylamine). Pale yellow oil, yield 135 mg (74%). Purity (HPLC method 1): 97.1% (t_R = 18.7 min). Specific rotation: $[\alpha]_D^{20} = -66.9$ (c = 1.05; CH_2Cl_2). MS (EM, APCI): *m*/*z* = calculated for $C_{20}H_{26}NO$ ($M + H^+$) 296.2009, found 296.2007. Further analytical data see (±)-**3a**.

4.3.25. N-benzyl-2-[(2S,6R)-6-phenyltetrahydropyran-2-yl] ethanamine ((2S,6R)-3a)

As described for (±)-**3a**, a mixture of (2*S*,6*R*)-**12** (175 mg, 0.61 mmol) and benzylamine (0.20 mL, 1.84 mmol) in acetonitrile (12 mL) was heated to reflux for 19 h. The residue was purified by flash column chromatography (Ø 3 cm, h 14 cm, 10 mL, cyclohexane:ethyl acetate = 7:1 + 1% dimethylethylamine). Pale yellow oil, yield 129 mg (72%). Purity (HPLC method 1): 98.2% (t_R = 18.6 min). Specific rotation: $[\alpha]_D^{20} = +68.7$ (c = 1.05; CH_2Cl_2). MS (EM, APCI): *m*/*z* = calculated for $C_{20}H_{26}NO$ ($M + H^+$) 296.2009, found 296.2001. Further analytical data see (±)-**3a**.

4.3.26. N-(Cyclohexylmethyl)-2-[(2R,6S)-6-phenyltetrahydropyran-2-yl]ethanamine ((2R,6S)-3b)

The mesylate (2*R*,6*S*)-**12** (138 mg, 0.49 mmol) was reacted with cyclohexylmethanamine (0.19 mL, 1.46 mmol) in acetonitrile (12 mL). The mixture was heated to reflux for 15.5 h, then the solvent was concentrated in vacuo and the residue was dissolved in ethyl acetate. The organic layer was extracted with 0.5 M NaOH (2 x), dried (Na_2SO_4) and filtered. The solvent was removed in vacuo and the product was purified by flash column chromatography (Ø 3 cm, h 14 cm, 10 mL, cyclohexane:ethyl acetate = 6:1 + 1% dimethylethylamine, R_f = 0.15). Pale yellow oil, yield 114 mg (77%). Purity (HPLC method 1): 97.4% (t_R = 19.9 min). Specific rotation: $[\alpha]_D^{20} = -60.5$ (c = 1.10; CH_2Cl_2). $C_{20}H_{31}NO$ (301.5 g/mol). MS (EI): *m*/*z* = 301 (M), 218 (M − C_6H_{11}), 175 (M − CH_2NR_2), 91 (CH_2Ph). MS (EM, APCI): *m*/*z* = calculated for $C_{20}H_{32}NO$ ($M + H^+$) 302.2478, found 302.2486. IR: $\tilde{\nu}$ (cm^{-1}) = 2919, 2848 (C—H), 1086, 1044 (C—O), 746, 696 (C-H_{arom}). ^1H NMR ($CDCl_3$): δ (ppm) = 0.75—0.88 (m, 2H, cyclohexane), 1.05—1.96 (m, 17H, CH(C*H*$_2$)$_3$CH—C*H*$_2$, cyclohexane), 2.37 (dd, J = 11.5/6.9 Hz, 1H, NHC*H*$_2$(C_6H_{11})), 2.42 (dd, J = 11.6/6.6 Hz, 1H, NHC*H*$_2$(C_6H_{11})), 2.73 (t, *J* = 6.8 Hz, 2H, CH_2CH_2NH), 3.55—3.61 (m, 1H, OC*H*R_2), 4.35 (dd, J = 11.3/2.2 Hz, 1H, PhC*H*), 7.21—7.39 (m, 5H, arom). A signal for the NH proton is not seen in the spectrum. ^{13}C NMR ($CDCl_3$): δ (ppm) = 24.0, 26.0, 26.1, 26.6, 31.3, 31.4, 31.5, 33.6, 36.5, 37.8 (10C, CH(CH_2)$_3$CH—CH_2, cyclohexane), 47.3 (1C, CH_2CH_2NH), 56.9 (1C, NHCH_2(C_6H_{11})), 77.7 (1C, OCHR_2), 79.6 (1C, Ph*C*H), 125.8 (2C, C-2, C-6 arom), 127.1 (1C, C-4 arom), 128.1 (2C, C-3, C-5 arom), 143.5 (1C, C-1 arom).

4.3.27. N-(Cyclohexylmethyl)-2-[(2S,6R)-6-phenyltetrahydropyran-2-yl]ethanamine ((2S,6R)-3b)

As described for (2*R*,6*S*)-**3b**, a solution of (2*S*,6*R*)-**12** (150 mg, 0.53 mmol) and cyclohexylmethanamine (0.20 mL, 1.58 mmol) in acetonitrile (12 mL) was heated to reflux for 15 h. The residue was purified by flash column chromatography (Ø 3 cm, h 15 cm, 10 mL, cyclohexane:ethyl acetate = 6:1 + 1% dimethylethylamine). Pale yellow oil, yield 124 mg (77%). Purity (HPLC method 1): 97.3% (t_R = 19.9 min). Specific rotation: $[\alpha]_D^{20} = +64.0$ (c = 1.10; CH_2Cl_2). MS (EM, APCI): *m*/*z* = calculated for $C_{20}H_{32}NO$ ($M + H^+$) 302.2478, found 302.2494. Further analytical data see (2*R*,6*S*)-**3b**.

4.3.28. 4-Phenyl-N-{2-[(2R,6S)-6-phenyltetrahydropyran-2-yl] ethyl}butan-1-amine ((2R,6S)-3c)

The mesylate (2*R*,6*S*)-**12** (151 mg, 0.53 mmol) was reacted with 4-phenylbutan-1-amine (0.25 mL, 1.59 mmol) in acetonitrile (12 mL) under reflux for 14.5 h. The solvent was removed in vacuo, the residue was dissolved in ethyl acetate and washed with 0.5 M NaOH (2 x). The organic layer was dried (Na_2SO_4), filtered and concentrated in vacuo. The crude product was purified by flash column chromatography (Ø 3 cm, h 16 cm, 10 mL, cyclohexane:ethyl acetate = 2:1 + 1% dimethylethylamine, R_f = 0.15). Pale yellow oil, yield 90 mg (50%). Purity (HPLC method 1): 96.4% (t_R = 20.6 min). Specific rotation: $[\alpha]_D^{20} = -53.7$ (c = 0.90; CH_2Cl_2). $C_{23}H_{31}NO$ (337.5 g/mol). MS (EI): *m*/*z* = 337 (M), 218 (M − $CH_2CH_2CH_2Ph$), 175 (M − CH_2NHR), 162 (M − $CHCH_2NR_2$), 91 (CH_2Ph). MS (EM, APCI): *m*/*z* = calculated for $C_{23}H_{32}NO$ ($M + H^+$) 338.2478, found 338.2515. IR: $\tilde{\nu}$ (cm^{-1}) = 2930, 2855 (C—H), 1086, 1043 (C—O), 744, 696 (C-H_{arom}). ^1H NMR ($CDCl_3$): δ (ppm) = 1.26—1.97 (m, 12H, CH(CH_2)$_3$CH—CH_2, $CH_2CH_2CH_2CH_2$),

2.55–2.63 (m, 4H, CH_2NHCH_2), 2.75 (t, J = 6.9 Hz, 2H, CH_2Ph), 3.55–3.61 (m, 1H, $OCHR_2$), 4.36 (dd, J = 11.3/2.1 Hz, 1H, PhC*H*), 7.14–7.36 (m, 10H, arom). A signal for the NH proton is not seen in the spectrum. ^{13}C NMR ($CDCl_3$): δ (ppm) = 24.0, 29.2, 29.7, 31.4, 33.6, 35.8, 36.5 (7C, $CH(CH_2)_3CH-CH_2$, $CH_2CH_2CH_2CH_2Ph$), 47.0 (1C, $CH_2NH(CH_2)_4$), 49.9 (1C, $NHCH_2CH_2CH_2CH_2$), 77.4 (1C, $OCHR_2$), 79.6 (1C, PhCH), 125.6 (1C, C-4 $arom_{(phenylbutyl)}$), 125.7 (2C, arom), 127.1 (1C, C-4 $arom_{(benzene)}$), 128.1, 128.2, 128.4 (6C, arom), 142.5 (1C, $arom_{(phenylbutyl)}$), 143.5 (1C, $arom_{(benzene)}$).

4.3.29. 4-Phenyl-N-{2-[(2S,6R)-6-phenyltetrahydropyran-2-yl] ethyl}butan-1-amine ((2S,6R)-3c)

As described for (2*R*,6*S*)-**3c**, a mixture of mesylate (2*S*,6*R*)-**12** (154 mg, 0.54 mmol) and 4-phenylbutan-1-amine (0.26 mL, 1.62 mmol) in acetonitrile (12 mL) was heated to reflux for 13.5 h. The residue was purified by flash column chromatography (Ø 3 cm, h 14 cm, 10 mL, cyclohexane:ethyl acetate = 2:1 + 1% dimethylethylamine). Pale yellow oil, yield 109 mg (60%). Purity (HPLC method 1): 96.1% (t_R = 20.6 min). Specific rotation: $[\alpha]_D^{20}$ = +54.0 (c = 0.90; CH_2Cl_2). MS (EM, APCI): m/z = calculated for $C_{23}H_{32}NO$ ($M + H^+$) 338.2478, found 338.2494. Further analytical data see (2*R*,6*S*)-**3c**.

4.3.30. N,N-Dimethyl-2-[(2R,6S)-6-phenyltetrahydropyran-2-yl] ethanamine ((2R,6S)-3d)

A solution of the mesylate (2*R*,6*S*)-**12** (149 mg, 0.53 mmol) in acetonitrile (6 mL) was transferred into a 10-mL microwave vessel and a 2 M solution of dimethylamine in THF (0.79 mL, 1.58 mmol) was added. The mixture was reacted in a microwave apparatus. Parameters for the microwave synthesis (power (max.): 200 W; pressure (max.): 8 bar; temperature (max.): 140 °C; reaction time: ramp time 5 min, hold time 15 min). After microwave irradiation, the solvent was removed in vacuo and the residue was dissolved in ethyl acetate. The organic layer was washed with 0.5 M NaOH (2 x), dried (Na_2SO_4), filtered and concentrated in vacuo. The product was purified by flash column chromatography (Ø 3 cm, h 13 cm, 10 mL, cyclohexane:ethyl acetate = 2:1 + 1% dimethylethylamine, R_f = 0.16). Colorless oil, yield 87 mg (70%). Purity (HPLC method 1): 99.3% (t_R = 15.3 min). Specific rotation: $[\alpha]_D^{20}$ = −71.7 (c = 1.05; CH_2Cl_2). $C_{15}H_{23}NO$ (233.4 g/mol). MS (EI): m/z = 233 (M), 91 (CH_2Ph), 77 (Ph). MS (EM, APCI): m/z = calculated for $C_{15}H_{24}NO$ ($M + H^+$) 234.1852, found 234.1878. IR: $\tilde{\nu}$ (cm^{-1}) = 2934, 2856, 2815, 2763 (C–H), 1081, 1042 (C–O), 749, 697 (C-H_{arom}). ^{1}H NMR ($CDCl_3$): δ (ppm) = 1.28–1.97 (m, 8H, $CH(CH_2)_3CH-CH_2$), 2.25 (s, 6H, $N(CH_3)_2$), 2.37–2.51 (m, 2H, $CH_2N(CH_3)_2$), 3.52–3.58 (m, 1H, $OCHR_2$), 4.36 (dd, J = 11.3/2.0 Hz, 1H, PhC*H*), 7.22–7.42 (m, 5H, arom).$\tilde{\nu}$ ^{13}C NMR ($CDCl_3$): δ (ppm) = 24.0, 31.4, 33.6, 34.5 (4C, $CH(CH_2)_3CH-CH_2$), 45.5 (2C, $N(CH_3)_2$), 56.2 (1C, $CH_2N(CH_3)_2$), 76.6 (1C, $OCHR_2$), 79.5 (1C, PhCH), 125.7 (2C, C-2, C-6 arom), 127.0 (1C, C-4 arom), 128.2 (2C, C-3, C-5 arom), 143.6 (1C, C-1 arom).

4.3.31. N,N-Dimethyl-2-[(2S,6R)-6-phenyltetrahydropyran-2-yl] ethanamine ((2S,6R)-3d)

As described for (2*R*,6*S*)-**3d**, a 2 M solution of dimethylamine in THF (0.83 mL, 1.65 mmol) was reacted with the mesylate (2*S*,6*R*)-**12** (156 mg, 0.55 mmol) in acetonitrile (6 mL) in a microwave apparatus. The product was purified by flash column chromatography (Ø 3 cm, h 14 cm, 10 mL, cyclohexane:ethyl acetate = 2:1 + 1% dimethylethylamine). Colorless oil, yield 85 mg (66%). Purity (HPLC method 1): 98.9% (t_R = 15.3 min). Specific rotation: $[\alpha]_D^{20}$ = +76.0 (c = 1.05; CH_2Cl_2). MS (EM, APCI): m/z = calculated for $C_{15}H_{24}NO$ ($M + H^+$) 234.1852, found 234.1877. Further analytical data see (2*R*,6*S*)-**3d**.

4.3.32. 1-{2-[(2RS,6SR)-6-Phenyltetrahydropyran-2-yl]ethyl} pyrrolidine ((±)-3e)

Pyrrolidine (0.05 mL, 0.65 mmol) was added to a solution of (±)-**12** (62 mg, 0.22 mmol) in acetonitrile (15 mL) and the mixture was heated to reflux for 19 h. The solvent was evaporated in vacuo and ethyl acetate was added. The resulting solution was washed with 0.5 M NaOH (2 x), dried (Na_2SO_4) and filtered. After removing the solvent in vacuo, the residue was purified by flash column chromatography (Ø 2.5 cm, h 15 cm, 10 mL, cyclohexane:ethyl acetate = 5:1 + 1% dimethylethylamine, R_f = 0.11). Colorless oil, yield 51 mg (90%). Purity (HPLC method 1): 97.9% (t_R = 16.8 min). $C_{17}H_{25}NO$ (259.4 g/mol). MS (ESI): m/z = 260 ($M + H^+$). IR: $\tilde{\nu}$ (cm^{-1}) = 2932, 2779 (C–H), 1085, 1044 (C–O), 749, 697 (C-H_{arom}). ^{1}H NMR ($CDCl_3$): δ (ppm) = 1.25–1.96 (m, 12H, $CH(CH_2)_3CH-CH_2$, $N(CH_2CH_2)_2$), 2.54–2.70 (m, 6H, $CH_2N(CH_2CH_2)_2$), 3.52–3.58 (m, 1H, $OCHR_2$), 4.36 (dd, J = 11.3/2.1 Hz, 1H, PhC*H*), 7.22–7.40 (m, 5H, arom). ^{13}C NMR ($CDCl_3$): δ (ppm) = 23.4 (2C, $N(CH_2CH_2)_2$), 24.1, 31.4, 33.7, 36.0 (4C, $CH(CH_2)_3CH-CH_2$), 53.0 (1C, $CH_2N(CH_2CH_2)_2$), 54.3 (2C, $N(CH_2CH_2)_2$), 76.9 (1C, $OCHR_2$), 79.4 (1C, PhCH), 125.7 (2C, C-2, C-6 arom), 127.0 (1C, C-4 arom), 128.1 (2C, C-3, C-5 arom), 143.7 (1C, C-1 arom).

4.3.33. 1-{2-[(2R,6S)-6-Phenyltetrahydropyran-2-yl]ethyl} pyrrolidine ((2R,6S)-3e)

As described for (±)-**41**, the mesylate (2*R*,6*S*)-**39** (135 mg, 0.48 mmol) was reacted with $pyrrolidine_{(dest)}$ (0.12 mL, 1.43 mmol) in acetonitrile (12 mL) for 18 h. The product was purified by flash column chromatography (Ø 3 cm, h 14 cm, 10 mL, cyclohexane:ethyl acetate = 5:1 + 1% dimethylethylamine). Pale yellow oil, yield 109 mg (88%). Purity (HPLC method 1): 98.7% (t_R = 16.8 min). Specific rotation: $[\alpha]_D^{20}$ = −68.4 (c = 1.12; CH_2Cl_2). MS (EM, APCI): m/z = calculated for $C_{17}H_{26}NO$ ($M + H^+$) 260.2009, found 260.2009. Further analytical data see (±)-**3e**.

4.3.34. 1-{2-[(2S,6R)-6-Phenyltetrahydropyran-2-yl]ethyl} pyrrolidine ((2S,6R)-3e)

As described for (±)-**3e**, a solution of (2*S*,6*R*)-**12** (157 mg, 0.55 mmol) and $pyrrolidine_{(dest)}$ (0.14 mL, 1.65 mmol) in acetonitrile (12 mL) was heated to reflux for 21 h. The residue was purified by flash column chromatography (Ø 3 cm, h 13 cm, 10 mL, cyclohexane:ethyl acetate = 5:1 + 1% dimethylethylamine). Pale yellow oil, yield 133 mg (93%). Purity (HPLC method 1): 99.3% (t_R = 16.8 min). Specific rotation: $[\alpha]_D^{20}$ = +66.4 (c = 1.12; CH_2Cl_2). MS (EM, APCI): m/z = calculated for $C_{17}H_{26}NO$ ($M + H^+$) 260.2009, found 260.2015. Further analytical data see (±)-**3e**.

4.3.35. 1-Phenyl-4-{2-[(2R,6S)-6-phenyltetrahydropyran-2-yl] ethyl}piperazine((2R,6S)-3f)

1-Phenylpiperazine (0.21 mL, 1.41 mmol) was added to a solution of (2*R*,6*S*)-**12** (134 mg, 0.47 mmol) in acetonitrile (12 mL) and the mixture was heated to reflux for 14 h. Then the solvent was evaporated in vacuo and the residue was dissolved in ethyl acetate. The organic layer was washed with 0.5 M NaOH (2 x), dried (Na_2SO_4) and filtered. After removing the solvent in vacuo, the product was purified by flash column chromatography (Ø 3 cm, h 16 cm, 10 mL, cyclohexane:ethyl acetate = 7:1 + 1% dimethylethylamine, R_f = 0.21). Colorless solid, mp 65 °C, yield 153 mg (93%). Purity (HPLC method 1): 99.8% (t_R = 19.7 min). Specific rotation: $[\alpha]_D^{20}$ = −54.4 (c = 1.17; CH_2Cl_2). $C_{23}H_{30}N_2O$ (350.5 g/mol). MS (EI): m/z = 350 (M), 175 ($M - R_2NCH_2$), 162 ($M - CHCH_2NR_2$), 91 (CH_2Ph). MS (EM, APCI): m/z = calculated for $C_{23}H_{31}N_2O$ ($M + H^+$) 351.2431, found 351.2393. IR: $\tilde{\nu}$ (cm^{-1}) = 2934, 2817 (C–H), 1081, 1041 (C–O), 752, 691 (C-H_{arom}). ^{1}H NMR ($CDCl_3$): δ (ppm) = 1.26–1.53 (m, 2H, pyran), 1.64–1.98 (m, 6H, pyran,

CH_2CH_2N), 2.49–2.69 (m, 6H, $CH_2N(CH_2CH_2)_2N$), 3.22 (t, J = 4.9 Hz, 4H, $N(CH_2CH_2)_2NPh$), 3.54–3.60 (m, 1H, $OCHR_2$), 4.37 (dd, J = 11.3/2.1 Hz, 1H, PhCH), 6.85 (tt, J = 7.3/0.9 Hz, 1H, $arom_{(phenylpiperazine)}$ para), 6.93 (m, 2H, $arom_{(phenylpiperazine)}$ ortho), 7.21–7.40 (m, 7H, arom). ^{13}C NMR ($CDCl_3$): δ (ppm) = 24.0, 31.4, 33.7, 33.8 (4C, $CH(CH_2)_3CH-CH_2$), 49.1 (2C, $N(CH_2CH_2)_2NPh$), 53.3 (2C, $CH_2N(CH_2CH_2)_2N$), 55.1 (1C, $CH_2N(CH_2CH_2)_2N$), 78.8 (1C, $OCHR_2$), 79.5 (1C, PhCH), 116.0 (2C, C-2, C-6 $arom_{(phenylpiperazine)}$), 119.6 (1C, C-4 $arom_{(phenylpiperazine)}$), 125.7 (2C, arom), 127.0 (1C, C-4 $arom_{(benzene)}$), 128.2, 129.1 (4C, arom), 143.6 (1C, C-1, $arom_{(benzene)}$), 151.3 (1C, C-1 $arom_{(phenylpiperazine)}$).

4.3.36. 1-Phenyl-4-{2-[(2S,6R)-6-phenyltetrahydropyran-2-yl] ethyl}piperazine ((2S,6R)-3f)

As described for (2*R*,6*S*)-**3f**, (2*S*,6*R*)-**12** (145 mg, 0.51 mmol) was reacted with 1-phenylpiperazine (0.23 mL, 1.53 mmol) in acetonitrile (12 mL) for 17 h. The crude product was purified by flash column chromatography (Ø 3 cm, h 14 cm, 10 mL, cyclohexane:ethyl acetate = 7:1 + 1% dimethylethylamine). Colorless solid, yield 166 mg (93%). Purity (HPLC method 1): 98.9% (t_R = 19.7 min). Specific rotation: $[\alpha]_D^{20}$ = +54.8 (c = 1.17; CH_2Cl_2). MS (EM, APCI): m/z = calculated for $C_{23}H_{31}N_2O$ ($M + H^+$) 351.2431, found 351.2394. Further analytical data see (2*R*,6*S*)-**3f**.

4.3.37. 2-[(2R,6S)-6-phenyltetrahydropyran-2-yl]ethanamine ((2R,6S)-3g)

The benzylamine (2*R*,6*S*)-**3a** (85 mg, 0.29 mmol) was dissolved in THF (18 mL) and filled in a pressure vessel. Pd/C (10%, 27 mg) was added and the mixture was placed in a hydrogenation apparatus, where it was reacted with H_2 under pressure (5 bar). After 20 h, an additional amount of Pd/C (10%, 10 mg) was added and the mixture was again reacted with H_2 under pressure (5 bar) for 24 h. Then the mixture was filtered through Celite®, washed with ethyl acetate and the solvent was removed under vacuum. The product was purified by flash column chromatography twice (1. Ø 1 cm, h 14 cm, 5 mL, CH_2Cl_2:methanol = 9.5:0.5 + 1% dimethylethylamine, R_f = 0.32, 2. Ø 1 cm, h 15 cm, 5 mL, CH_2Cl_2:methanol = 1:1, R_f = 0.13). Yellow oil, yield 37 mg (61%). Purity (HPLC method 1): 91.5% (t_R = 14.3 min). Specific rotation: $[\alpha]_D^{20}$ = −81.5 (c = 0.65; CH_2Cl_2). $C_{13}H_{19}NO$ (205.3 g/mol). MS (EI): m/z = 205 (M), 91 (CH_2-Ph), 72 (C_4H_8O). MS (EM, APCI): m/z = calculated for $C_{13}H_{20}NO$ ($M + H^+$) 206.1539, found 206.1573. IR: $\tilde{\nu}$ (cm^{-1}) = 2932, 2854 (C–H), 1085, 1041 (C–O), 749, 697 (C-H_{arom}). ^1H NMR ($CDCl_3$): δ (ppm) = 1.30–1.97 (m, 10H, $CH(CH_2)_3CH-CH_2$, NH_2), 2.86 (t, J = 6.8 Hz, 2H, CH_2NH_2), 3.58–3.64 (m, 1H, $OCHR_2$), 4.36 (dd, J = 11.3/2.1 Hz, 1 H, PhCH), 7.22–7.39 (m, 5H, arom). ^{13}C NMR ($CDCl_3$): δ (ppm) = 24.0, 31.4, 33.6 (3C, pyran), 39.1 (1C, $CH_2CH_2NH_2$), 39.3 (1C, CH_2NH_2), 77.1 (1C, $OCHR_2$), 79.7 (1C, PhCH), 125.7 (2C, C-2, C-6 arom), 127.1 (1C, C-4 arom), 128.2 (2C, C-3, C-5 arom), 143.3 (1C, C-1 arom).

4.3.38. 2-[(2S,6R)-6-phenyltetrahydropyran-2-yl]ethanamine ((2S,6R)-3g)

As described for (2*R*,6*S*)-**3g**, a mixture of (2*S*,6*R*)-**3a** (78 mg, 0.26 mmol) and Pd/C (10%, 31 mg) in THF (14 mL) was reacted with H_2 under pressure (5 bar) for 29 h, without a second addition of Pd/C. The product was purified by flash column chromatography twice (1. Ø 1 cm, h 15 cm, 5 mL, CH_2Cl_2:methanol = 9:1, R_f = 0.08, 2. Ø 1 cm, h 18 cm, 5 mL, CH_2Cl_2:methanol = 9.5:0.5 + 1% dimethylethylamine). Yellow oil, yield 23 mg (42%). Purity (HPLC method 1): 94.4% (t_R = 14.3 min). Specific rotation: $[\alpha]_D^{20}$ = +81.6 (c = 0.65; CH_2Cl_2). MS (EM, APCI): m/z = calculated for $C_{13}H_{20}NO$ ($M + H^+$) 206.1539, found 206.1567. Further analytical data see (2*R*,6*S*)-**3g**.

4.4. Receptor binding studies

4.4.1. General procedures for the binding assays

The test compound solutions were prepared by dissolving approximately 10 μmol (usually 2–4 mg) of test compound in DMSO so that a 10 mM stock solution was obtained. To obtain the required test solutions for the assay, the DMSO stock solution was diluted with the respective assay buffer. The filtermats were presoaked in 0.5% aqueous polyethylenimine solution for 2 h at rt before use. All binding experiments were carried out in duplicates in the 96 well multiplates. The concentrations given are the final concentration in the assay. Generally, the assays were performed by addition of 50 μL of the respective assay buffer, 50 μL of test compound solution in various concentrations (10^{-5}, 10^{-6}, 10^{-7}, 10^{-8}, 10^{-9} and 10^{-10} mol/L), 50 μL of the corresponding radioligand solution and 50 μL of the respective receptor preparation into each well of the multiplate (total volume 200 μL). The receptor preparation was always added last. During the incubation, the multiplates were shaken at a speed of 500–600 rpm at the specified temperature. Unless otherwise noted, the assays were terminated after 120 min by rapid filtration using the harvester. During the filtration, each well was washed five times with 300 μL of water. Subsequently, the filtermats were dried at 95 °C. The solid scintillator was melted on the dried filtermats at a temperature of 95 °C for 5 min. After solidifying of the scintillator at rt, the trapped radioactivity in the filtermats was measured with the scintillation analyzer. Each position on the filtermat corresponding to one well of the multiplate was measured for 5 min with the [^{3}H]-counting protocol. The overall counting efficiency was 20%. The IC_{50} values were calculated with the program GraphPad Prism® 3.0 (GraphPad Software, San Diego, CA, USA) by non-linear regression analysis. Subsequently, the IC_{50} values were transformed into K_i values using the equation of Cheng and Prusoff [61]. The K_i values are given as mean value ± SEM from three independent experiments.

4.4.2. σ_1 receptor assay

The assay was performed with the radioligand [^{3}H]-(+)-pentazocine (22.0 Ci/mmol; PerkinElmer). The thawed membrane preparation of guinea pig brain (about 100 μg of the protein) was incubated with various concentrations of test compounds, 2 nM [^{3}H]-(+)-pentazocine, and TRIS buffer (50 mM, pH 7.4) at 37 °C. The non-specific binding was determined with 10 μM unlabeled (+)-pentazocine. The K_d value of (+)-pentazocine is 2.9 nM [62].

4.5. Computational details

4.5.1. General

The starting structure for the σ_1 receptor was obtained from the RCSB Protein Data Bank (PDB ID 5HK1) [34], of which only the protomer with the more complete sequence was retained for the simulations. All docking experiments were performed with Autodock 4.3/Autodock Tools 1.4.6 [63]on a win64 platform. A total of 300 Monte Carlo/simulated annealing (MC/SA) runs were performed, with 100 constant-temperature cycles for simulated annealing. The structures of all compounds were subjected to cluster analysis with a 1 Å tolerance for an all-atom root-mean-square (rms) deviation from a lower energy structure representing each cluster family. The resulting docked conformations were clustered and visualized; then, for each compound, only the molecular conformation satisfying the combined criteria of having the lowest (i.e., more favorable) Autodock energy and belonging to a highly populated cluster was selected to carry for further modeling.

The CHARMM-GUI server [64] was used to embed the σ_1/ligand complex in a palmitoyl-oleyl-phosphatidyl-choline (POPC, 218 lipid

molecules were added) bilayer solvated with explicit TIP3P [65] water molecules to succeed complete hydration of the membrane and reach a physiological concentration of sodium and chloride ions (0.15 M NaCl). Antechamber program from AMBER19 [58] was used to assign gaff2 [66] atom types to each ligand, while ligand's partial charges were derived by employing the RESP method offered by the RED server [67]. Classical Molecular Dynamics simulations on σ_1 receptor in complex with the new tetrahydropyran derivatives are carried out following a well validated procedure [42,68,69]. Briefly, the system density and volume were relaxed in NPT ensemble maintaining the Berendsen barostat for 20 ns. After this step, 50 ns of unrestrained NVT production simulation was run for each system. All images were created by the UCSF Chimera software [70], and graphs were produced by GraphPad Prism 8 (GraphPad Software, San Diego, California USA, www.graphpad.com).

4.5.2. Free energy perturbation (FEP)

The final structure obtained from the unrestrained simulation for each system with cyclohexane-based ligand was used as the starting configuration for the subsequent FEP simulations in the ansatz of alchemical free energy (AFE) studies with the thermodynamic integration module implemented in pmemd from AMBER19. In order to compute the difference in binding energy between analogous cyclohexane (**2**) and tetrahydropyran ligands (**3**), each cyclohexane derivative was gradually mutated to its corresponding tetrahydropyran derivative in 16 equally spaced lambda windows. The softcore Lennard-Jones and electrostatic potential were used to allow for a single step approach [71]. Hydrogen mass repartitioning implemented in AMBER19 was used to allow a 4 fs integration time step [72]. To speed-up convergence, the Hamiltonian replica exchange molecular dynamic (H-REMD) was employed, allowing exchanges from neighboring replicas during the AFE simulation. In total, for each lambda window 7500 exchanges were attempted, with 8 ps elapsed between exchange for a total of 60 ns of simulation for each replica. The tool *alchemical_analysis.py* from https://github.com/MobleyLab/alchemical-analysis [73] was used to analyze the data obtained from the AFE simulations, allowing to remove correlated data and discard for each simulated window the first ~30 ns of data as equilibration. The multistate Bennett acceptance ratio (MBAR [74]) estimator was used to get the final ΔG_{FEP} values.

4.5.3. Steered molecular dynamic (SMD) calculations

The final structure obtained from the unrestrained simulation for each σ_1 ligand complex was used as starting configuration for the constant velocity steered molecular dynamics (CV-SMD) unbinding simulations. The pathway chosen for the unbinding process was the one going towards the solvent, as it was found the preferred unbound pathway from Rossino et al. [75]. A pulling spring with a force constant of 5 kcal/mol Å^2 was applied to the ligand center of mass and moved at a constant velocity of 5×10^{-6} Å/ps along the unbinding direction. The simulations were carried out until the ligands were completely unbound form the receptor and the force acting on the ligands was monitored to obtain its profile along the unbinding direction.

4.6. Capsaicin assay, antiallodynic activity

In vivo efficacy studies in mice were conducted at the University of Granada, Granada, Spain. Animal care was provided in accordance with institutional (Research Ethics Committee of the University of Granada, Granada, Spain), regional (Junta de Andalucía, Spain), and international standards (European Communities Council Directive 2010/63). The protocol of the experiments was approved by the Research Ethics Committee of the University of Granada (Licence 2010−322).

Female CD-1 mice (Charles River, Barcelona, Spain) weighing 25−30 g were used for all experiments. The animals were housed in a temperature-controlled room (21 ± 1 °C) with air exchange every 20 min and an automatic 12 h light/dark cycle (8−20 h). They were fed a standard laboratory diet and tap water ad libitum until the beginning of the experiments. The experiments were performed during the light phase (9−15 h).

To evaluate the effect of drugs on mechanical allodynia induced by capsaicin, a previously described experimental procedure was used [24]. The compound under study or its solvent (HPMC) was administered s.c. to mice 30 min before the intraplantar (i.pl.) administration of 20 μL capsaicin (1 μg in 1% DMSO). 15 min after the i.pl. administration of capsaicin, a mechanical punctate stimulation (0.5 g force) was applied with an electronic von Frey device (Dynamic Plantar Aesthesiometer, Ugo Basile, Comerio, Italy) at least 5 mm from the site of injection toward the toes (area of secondary mechanical hypersensitivity), and the paw withdrawal latency time was automatically recorded. Each mouse was tested in three trials at 30 s intervals and the mean of the 3 measurements was calculated. A cutoff time of 50 s was used in each trial.

The degree of effect on capsaicin-induced mechanical allodynia was calculated as:

% antiallodynic effect = [(LTD-LTS)/(CT-LTS)] x 100 where LTD is the latency time for paw withdrawal in drug-treated animals, LTS is the latency time in solvent-treated animals (mean value 12.03 s), and CT is the cutoff time (50 s).

Declaration of competing interest

The authors declare no conflict of interest.

Acknowledgements

This work was supported by the Deutsche Forschungsgemeinschaft *(DFG),* which is gratefully acknowledged. We thank Prof. Dr. S. Grimme for calculating the CD spectra.

List of abbreviations

CBS	Corey-Bakshi-Shibata
CD	circular dichroism
CIP	Cahn-Ingold-Prelog
CNS	central nervous system
CYP	cytochrome P450
3D	three dimensional
DIBAL	diisobutylaluminum hydride
DIP-Cl	Ipc_2BCl, B-Chlordiisopinocampheylborane
DMSO	dimethyl sulfoxide
ee	enantiomeric excess
ER	endoplasmic reticulum
FEP	free energy perturbation
HPLC	high performance lipid chromatography
MD	molecular dynamics
NMDA	N-methyl-D-aspartate
NOE	nuclear Overhauser effect
PCP	1-(1-phenylcyclohexyl)piperidine, phencyclidine
PDB	protein data bank
SMD	steered molecular dynamics
TBME	*tert*-butyl methyl ether
TMEM97	transmembrane protein 97

Appendix A. Supplementary data

Supplementary data to this article can be found online at https://doi.org/10.1016/j.ejmech.2021.113443.

References

[1] W.R. Martin, C.G. Eades, J.A. Thompson, R.E. Huppler, P.E. Gilbert, The effects of morphine- and nalorphine- like drugs in the nondependent and morphine-dependent chronic spinal dog, J. Pharmacol. Exp. Therapeut. 197 (1976) 517–532.

[2] B.D. Vaupel, Naltrexone fails to antagonize the σ-effects of PCP and SKF 10,047 in the dog, Eur. J. Pharmacol. 92 (1983) 269–274.

[3] S.B. Hellewell, W.D. Bowen, A sigma-like binding site in rat pheochromocytoma (PC12) cells: decreased affinity for (+)-benzomorphans and lower molecular weight suggest a different sigma receptor form from that of Guinea pig brain, Brain Res. 527 (1990) 244–253.

[4] S.B. Hellewell, A. Bruce, G. Feinstein, J. Orringer, W. Williams, W.D. Bowen, Rat liver and kidney contain high densities of sigma 1 and sigma 2 receptors: characterization by ligand binding and photoaffinity labeling, Eur. J. Pharmacol. 268 (1994) 9–18.

[5] D.C. Mash, C.P. Zabetian, Sigma receptors Are associated with cortical Limbic areas in the primate brain, Synapse 12 (3) (1992) 195–205.

[6] N.N. Samovilova, L.V. Nagornaya, V.A. Vinogradov, (+)-[H-3]Skf 10,047 binding-sites in rat-liver, Eur. J. Pharmacol. 147 (2) (1988) 259–264.

[7] J.M. Walker, W.D. Bowen, F.O. Walker, R.R. Matsumoto, B. Decosta, K.C. Rice, Sigma-receptors - biology and function, Pharmacol. Rev. 42 (4) (1990) 355–402.

[8] C.P. Zabetian, J.K. Staley, D.D. Flynn, D.C. Mash, [H-3]-(+)-Pentazocine binding to sigma-recognition sites in human rebellum, Life Sci. 55 (20) (1994) Pl389–Pl395.

[9] E.J. Cobos, J.M. Entrena, F.R. Nieto, C.M. Cendan, E. Del Pozo, Pharmacology and therapeutic potential of sigma(1) receptor ligands, Curr. Neuropharmacol. 6 (4) (2008) 344–366.

[10] T. Hayashi, S.Y. Tsai, T. Mori, M. Fujimoto, T.P. Su, Targeting ligand-operated chaperone sigma-1 receptors in the treatment of neuropsychiatric disorders, Expert Opin. Ther. Targets 15 (2011) 557–577.

[11] T. Hayashi, T.P. Su, sigma-1 receptor ligands – potential in the treatment of neuropsychiatric disorders, CNS Drugs 18 (5) (2004) 269–284.

[12] T. Maurice, T.P. Su, The pharmacology of sigma-1 receptors, Pharmacol. Ther. 124 (2) (2009) 195–206.

[13] S. Collina, R. Gaggeri, A. Marra, A. Bassi, S. Negrinotti, F. Negri, D. Rossi, Sigma receptor modulators: a patent review, Exp. Op. Ther. Pat. 23 (2013) 597–613.

[14] T. Ishima, Y. Fujita, K. Hashimoto, Interaction of new antidepressants with sigma-1 receptor chaperones and their potentiation of neurite outgrowth in PC12 cells, Eur. J. Pharmacol. 727 (2014) 167–173.

[15] F. Langa, X. Codony, V. Tovar, A. Lavado, E. Giménez, P. Cozar, M. Cantero, A. Dordal, E. Hernández, R. Pérez, X. Monroy, D. Zamanillo, X. Guitart, L. Montoliu, Generation and phenotypic analysis of sigma receptor type I (σ1) knockout mice, Eur. J. Neurosci. 18 (2003) 2188–2196.

[16] V. Sabino, P. Cottone, S.L. Parylak, L. Steardo, E.P. Zorrilla, Sigma-1 receptor knockout mice display a depressive-like phenotype, Behav. Brain Res. 198 (2009) 472–476.

[17] W.E. Müller, B. Siebert, G. Holoubek, C. Gentsch, Neurophamracology of the anxiolytic drug opripramol, a sigma site ligand, Pharmacopsychiatry 37 (3) (2004) 189–197.

[18] I. Hindmarch, K. Hashimoto, Cognition and depression: the effects of fluvoxamine, a sigma-1 receptor agonist, reconsidered, Hum. Psychopharmacol. Clin. Exp. 25 (2010) 193–200.

[19] J. Meunier, J. Ieni, T. Maurice, The anti-amnesic and neuroprotective effects of donepezil against amyloid $\beta_{25\text{-}35}$ peptide-induced toxicity in mice involve an interaction with the σ_1 receptor, Br. J. Pharmacol. 149 (2006) 998–1012.

[20] K. Kato, H. Hayako, Y. Ishihara, S. Marui, M. Iwane, M. Miyamoto, TAK-147, an acetylcholinesterase inhibitor, increases choline acetyltransferase activity in cultured rat septal cholinergic neurons, Neurosci. Lett. 260 (1999) 5–8.

[21] J.L. Diaz, R. Cuberes, J. Berrocal, M. Contijoch, U. Christmann, A. Fernandez, A. Port, J. Holenz, H. Buschmann, C. Laggner, M.T. Serafini, J. Burgueno, D. Zamanillo, M. Merlos, J.M. Vela, C. Almansa, Synthesis and biological evaluation of the 1-arylpyrazole class of σ(1) receptor antagonists: identification of 4-{2-[5-methyl-1-(naphthalen-2-yl)-1H-pyrazol-3-yloxy]ethyl} morpholine (S1RA, E-52862), J. Med. Chem. 55 (2012) 8211–8224.

[22] B. Wünsch, The σ_1 receptor antagonist S1RA is a promising candidate for the treatment of neurogenic pain, J. Med. Chem. 55 (2012) 8209–8210.

[23] I. Bravo-Caparrós, G. Perazzoli, S. Yeste, D. Cikes, J.M. Baeyens, E.J. Cobos, F.R. Nieto, Sigma-1 receptor inhibition reduces neuropathic pain induced by partial sciatic nerve transection in mice by opioid-dependent and -independent mechanisms, Front. Pharmacol. 10 (2019) 613.

[24] J.M. Entrena, E.J. Cobos, F.R. Nieto, C.M. Cendán, G. Gris, E. Del Pozo, D. Zamanillo, J.M. Baeyens, Sigma-1 receptors are essential for capsaicin-induced mechanical hypersensitivity: studies with selective sigma-1 ligands and sigma-1 knockout mice, Pain 143 (3) (2009) 252–261.

[25] A. Binder, Human surrogate models of neuropathic pain: validity and limitations [published correction] appears in, Pain 157 (7) (2016) 48–52.

[26] J. Entrena, C. Sánchez-Fernández, F. Nieto, Sigma-1 receptor agonism promotes mechanical allodynia after priming the nociceptive system with capsaicin, Sci. Rep. 6 (2016) 37835.

[27] E. Aydar, C.P. Palmer, M.B. Djamgoz, Sigma receptors and cancer: possible involvement of ion channels, Canc. Res. 64 (2004) 5029–5035.

[28] A. van Waarde, A.A. Rybczynska, N.K. Ramakrishnan, K. Ishiwata, P.H. Elsinga, R.A.J.O. Dierckx, Potential applications for sigma receptor ligands in cancer diagnosis and therapy, Biochim. Biophys. Acta 1848 (10) (2015) 2703–2714.

[29] M. Hanner, F.F. Moebius, A. Flandorfer, H.G. Knaus, J. Striessnig, E. Kempner, H. Glossmann, Purification, molecular cloning, and expression of the mammalian sigma1-binding site, Proc. Natl. Acad. Sci. U.S.A. 93 (1996) 8072–8077.

[30] R. Kekuda, P.D. Prasad, Y.J. Fei, F.H. Leibach, V. Ganapathy, Cloning and functional expression of the human type 1 sigma receptor (hSigmaR1), Biochem. Biophys. Res. Commun. 229 (1996) 553–558.

[31] P. Seth, F.H. Leibach, V. Ganapathy, Cloning and structural analysis of the cDNA and the gene encoding the murine type 1 sigma receptor, Biochem. Biophys. Res. Commun. 241 (1997) 535–540.

[32] P. Seth, Y.-J. Fei, H.W. Li, W. Huang, F.H. Leibach, V. Ganapathy, Cloning and functional characterization of a σ receptor from rat brain, J. Neurochem. 70 (1998) 922–931.

[33] P.D. Prasad, H.W. Li, Y.-J. Fei, M.E. Ganapathy, T. Fujita, L.H. Plumley, T.L. Yang-Feng, F.H. Leibach, V. Ganapathy, Exon-intron structure, analysis of promoter region, and chromosomal localization of the human type 1 σ receptor gene, J. Neurochem. 70 (1998) 443–451.

[34] H.R. Schmidt, S.D. Zheng, E. Gurpinar, A. Koehl, A. Manglik, A.C. Kruse, Crystal structure of the human sigma 1 receptor, Nature 532 (7600) (2016) 527–530.

[35] H.R. Schmidt, R.M. Betz, R.O. Dror, A.C. Kruse, Structural basis for sigma(1) receptor ligand recognition, Nat. Struct. Mol. Biol. 25 (10) (2018) 981–987.

[36] A. Alon, H.R. Schmidt, M.D. Wood, J.J. Sahn, S.F. Martin, A.C. Kruse, Identification of the gene that codes for the σ2 receptor, Proc. Natl. Acad. Sci. U.S.A. 114 (2017) 7160–7165.

[37] M. Ishikawa, K. Hashimoto, The role of sigma-1 receptors in the pathophysiology of neuropsychiatric diseases, J. Recept. Ligand Channel Res. 3 (2010) 25–36.

[38] T.L. Collier, R.N. Waterhouse, M. Kassiou, Imaging sigma receptors: applications in drug development, Curr. Pharmacol. Design 13 (2007) 51–72.

[39] T. Utech, J. Köhler, B. Wünsch, Synthesis of 4-(aminoalkyl) subsituted 1,3-dioxanes as potent NMDA and σ receptor antagonists, Eur. J. Med. Chem. 46 (2011) 2157–2169.

[40] T. Utech, J. Köhler, H. Buschmann, J. Holenz, J.M. Vela, B. Wünsch, Synthesis and pharmacological evaluation of a potent and selective σ_1 receptor antagonist with high antiallodynic activity, Arch. Pharm. Chem. Life Sci. 344 (2011) 415–421.

[41] J. Köhler, K. Bergander, J. Fabian, D. Schepmann, B. Wünsch, Enantiomerically pure 1,3-dioxanes as highly selective NMDA and σ_1 receptor ligands, J. Med. Chem. 55 (2012) 8953–8957.

[42] N. Kopp, C. Holtschulte, F. Börgel, K. Lehmkuhl, K. Friedland, G. Civenni, E. Laurini, C.V. Catapano, S. Pricl, H.-U. Humpf, D. Schepmann, B. Wünsch, Novel σ_1 antagonists designed for tumor therapy: structure - activity relationships of aminoethyl substituted cyclohexanes, Eur. J. Med. Chem. 210 (2021) 112950.

[43] F. Galla, C. Bourgeois, K. Lehmkuhl, D. Schepmann, M. Soeberdt, T. Lotts, C. Abels, S. Ständer, B. Wünsch, Effects of polar κ receptor agonists designed for the periphery on ATP-induced Ca2+ release from keratinocytes, Med. Chem. Commun. 7 (2016) 317–326.

[44] V. Butsch, F. Börgel, F. Galla, K. Schwegmann, S. Hermann, M. Schäfers, B. Riemann, B. Wünsch, S. Wagner, Design, (Radio)Synthesis, and in vitro and in vivo evaluation of highly selective and potent matrix metalloproteinase (MMP-12) inhibitors as radiotracers for positron emission tomography, J. Med. Chem. 61 (2018) 4115–4134.

[45] J. Köhler, B. Wünsch, Computer simulation of asymmetric transformations, Tetrahedron: Asymmetry 17 (2006) 3100–3110.

[46] R. Downham, P.J. Edwards, D.A. Entwistle, A.B. Hughes, K.S. Kim, S.V. Ley, Dispiroketals in synthesis (part 19)[1]: dispiroketals as enantioselective and regioselective protective agents for symmetric cyclic and acyclic polyols, Tetrahedron: Asymmetry 6 (1995) 2403–2440.

[47] P.V. Ramachandran, S. Pitre, H.C. Brown, Selective reductions. 59. Effective intramolecular asymmetric reductions of α-, β-, and γ-keto acids with diisopinocampheylborane and intermolecular asymmetric reductions of the corresponding esters with B-chlorodiisopinocampheylborane, J. Org. Chem. 67 (2002) 5315–5319.

[48] E. Francotte, R.M. Wolf, Preparation of chiral building blocks and auxiliaries by chromatography on cellulose triacetate (CTA I): indications for the presence of multiple interaction sites in CTA I, Chirality 2 (1990) 16–31.

[49] J. Hsu, J. Fang, Stereoselective synthesis of δ-lactones from 5-oxoalkanals via one-pot sequential acetalization, tishchenko reaction, and lactonization by cooperative catalysis of samarium ion and mercaptan, J. Org. Chem. 66 (2001) 8573–8584.

[50] G. Blay, V. Hernandez-Olmos, J.R. Pedro, Enantioselective henry addition of methyl 4-nitrobutyrate to aldehydes. Chiral building blocks for 2-pyrrolidinones and other derivatives, Org. Lett. 12 (2010) 3058–3061.

[51] V. Nair, J. Prabhakaran, T.G. George, A facile synthesis of optically active lactones using benzyl-3,6-anhydro glucofuranoside as chiral auxiliary, Tetrahedron 53 (1997) 15061–15068.

[52] A. Kamal, M. Sandbhor, A.A. Shaik, Application of a one-pot lipase resolution strategy for the synthesis of chiral γ- and δ-lactones, Tetrahedron: Asymmetry 14 (2003) 1575–1580.
[53] T. Izumi, F. Tamura, M. Akutsu, Enzymatic resolution of 4-methyl-, 4-phenyl- and 6-phenyltetrahydro-2H-pyran-2-one using esterases, J. Heterocycl. Chem. 31 (1994) 441–445.
[54] R.J. Kazlauskas, A.N.E. Weissfloch, A.T. Rappaport, L.A. Cuccia, A rule to predict which enantiomer of a secondary alcohol reacts faster in reactions catalyzed by cholesterol esterase, lipase from Pseudomonas cepacia, and lipase from Candida rugose, J. Org. Chem. 56 (1991) 2656–2665.
[55] P. Hasebein, B. Frehland, K. Lehmkuhl, R. Fröhlich, D. Schepmann, B. Wünsch, Synthesis and pharmacological evaluation of like- and unlike-configured tetrahydro-2-benzazepines with the α-substituted benzyl moiety in the 5-position, Org. Biomol. Chem. 12 (2014) 5407–5426.
[56] C. Meyer, B. Neue, D. Schepmann, S. Yanagisawa, J. Yamaguchi, E.-W. Würthwein, K. Itami, B. Wünsch, Improvement of σ1 receptor affinity by late-stage C-H-bond arylation of spirocyclic lactones, Bioorg. Med. Chem. 21 (2013) 1844–1856.
[57] K. Miyata, D. Schepmann, B. Wünsch, Synthesis and σ receptor affinity of regioisomeric spirocyclic furopyridines, Eur. J. Med. Chem. 83 (2014) 709–716.
[58] D.A. Case, I.Y. Ben-Shalom, S.R. Brozell, D.S. Cerutti, T.E. Cheatham III, V.W.D. Cruzeiro, T.A. Darden, R.E. Duke, D. Ghoreishi, G. Giambasu, T. Giese, M.K. Gilson, H. Gohlke, A.W. Goetz, D. Greene, R. Harris, N. Homeyer, Y. Huang, S. Izadi, A. Kovalenko, R. Krasny, T. Kurtzman, T.S. Lee, S. LeGrand, P. Li, C. Lin, J. Liu, T. Luchko, R. Luo, V. Man, D.J. Mermelstein, K.M. Merz, Y. Miao, G. Monard, C. Nguyen, H. Nguyen, A. Onufriev, F. Pan, R. Qi, D.R. Roe, A.E. Roitberg, C. Sagui, S. Schott-Verdugo, J. Shen, C.L. Simmerling, J. Smith, J. Swails, R.C. Walker, J. Wang, H. Wei, L. Wilson, R.M. Wolf, X. Wu, L. Xiao, Y. Xiong, D.M. York, P.A. Kollman, AMBER 2019, University of California, San Francisco, 2019.
[59] K.R. Stone, D.D. Mickey, H. Wunderli, G.H. Mickey, D.F. Paulson, Isolation of a human prostate carcinoma cell line (DU 145), Int. J. Canc. 21 (1978) 274–281.
[60] R. Vazquez, G. Civenni, A. Kokanovic, D. Shinde, J. Cantergiani, M. Marchetti, G. Zoppi, B. Ruggeri, P.C.C. Liu, G.M. Carbone, V.V. Catapano, Efficacy of novel bromodomain and extraterminal inhibitors in combination with chemotherapy for castration-resistant prostate cancer, Eur. Urol. Oncol. (2019).
[61] Y.-C. Cheng, W.H. Prusoff, Relationship between the inhibition constant (KI) and the concentration of inhibitor which causes 50 per cent inhibition (I50) of an enzymatic reaction, Biochem. Pharmacol. 22 (1973) 3099–3108.
[62] D.L. DeHaven-Hudkins, L.C. Fleissner, F.Y. Ford-Rice, Characterization of the binding of [^{3}H](+)-pentazocine to σ recognition sites in Guinea pig brain, Eur. J. Pharmacol. Mol. Pharmacol. 227 (1992) 371–378.
[63] G.M. Morris, R. Huey, W. Lindstrom, M.F. Sanner, R.K. Belew, D.S. Goodsell, A.J. Olson, AutoDock4 and AutoDockTools4: automated docking with selective receptor flexibility, J. Comput. Chem. 30 (2009) 2785–2791.
[64] J. Sunhwan, K. Taehoon, G.I. Vidyashankara, I. Wonpil, CHARMM-GUI: a web-based graphical user interface for CHARMM, J. Comput. Chem. 11 (2008) 1859–1865.
[65] W.L. Jorgensen, J. Chandrasekhar, J.D. Madura, R.W. Impey, M.L. Klein, Comparison of simple potential functions for simulating liquid water, J. Chem. Phys. 79 (1983) 926–935.
[66] W. Junmei, M.W. Romain, W.C. James, A.K. Peter, A.C. David, Development and testing of a general amber force field, J. Comput. Chem. 25 (9) (2004) 1157–1174.
[67] E. Vanquelef, S. Simon, G. Marquant, E. Garcia, G. Klimerak, J.C. Delepine, P. Cieplak, F.-Y. Dupradeau, R.E.D. Server, A web service for deriving RESP and ESP charges and building force field libraries for new molecules and molecular fragments, Nucleic Acids Res. 39 (suppl_2) (2011) W511–W517.
[68] M.E. Valencia, C. Herrera-Arozamena, L. de Andres, C. Perez, J.A. Morales-Garcia, A. Perez-Castillo, E. Ramos, A. Romero, D. Viña, M. Yañez, E. Laurini, S. Pricl, M.I. Rodriguez-Franco, Neurogenic and neuroprotective donepezil-flavonoid hybrids with sigma-1 affinity and inhibition of key enzymes in Alzheimer's disease, Eur. J. Med. Chem. 156 (2018) 534–553.
[69] E. Kronenberg, F. Weber, S. Brune, D. Schepmann, C. Almansa, K. Friedland, E. Laurini, S. Pricl, B. Wünsch, Synthesis and Structure–Affinity relationships of spirocyclic benzopyrans with exocyclic amino moiety, J. Med. Chem. 62 (2019) 4204–4217.
[70] E.F. Pettersen, T.D. Goddard, C.C. Huang, G.S. Couch, D.M. Greenblatt, E.C. Meng, T.E. Ferrin, UCSF Chimera–a visualization system for exploratory research and analysis, J. Comput. Chem. 25 (13) (2004) 1605–1612.
[71] T. Steinbrecher, D.L. Mobley, D.A. Case, Onlinear scaling schemes for Lennard-Jones interactions in free energy calculations, J. Chem. Phys. 127 (21) (2007) 214108.
[72] C.W. Hopkins, S. Le Grand, R.C. Walker, A.E. Roitberg, Long-time-step molecular dynamics through hydrogen mass repartitioning, J. Chem. Theor. Comput. 11 (4) (2015) 1864–1874.
[73] P.V. Klimovich, M.R. Shirts, D.L. Mobley, Guidelines for the analysis of free energy calculations, J. Comput. Aided Mol. Des. 29 (5) (2015) 397–411.
[74] M.R. Shirts, J.D. Chodera, Statistically optimal analysis of samples from multiple equilibrium states, J. Chem. Phys. 129 (12) (2008) 124105.
[75] G. Rossino, I. Orellana, J. Caballero, D. Schepmann, B. Wunsch, M. Rui, D. Rossi, M. Gonzalez-Avendano, S. Collina, A. Vergara-Jaque, New insights into the opening of the occluded ligand-binding pocket of Sigma1 receptor: binding of a novel bivalent RC-33 derivative, J. Chem. Inf. Model. 60 (2) (2020) 756–765.